GEOPHYSICS, VOL. 64, NO. 3 (MAY-JUNE 1999); P. 820–837, 11 FIGS., 1 TABLE.

3-D moveout velocity analysis and parameter estimation for orthorhombic media

Vladimir Grechka* and Ilya Tsvankin*

ABSTRACT

Orthorhombic symmetry describes several azimuthally anisotropic models typical for fractured formations, such as those containing two orthogonal crack systems or parallel vertical cracks in a VTI (transversely isotropic with a vertical symmetry axis) background. Here, we present a methodology for inverting multiazimuth P-wave reflection traveltimes for the parameters of vertically inhomogeneous orthorhombic media. Our approach is based on the general analytic representation of normal-moveout (NMO) velocity as an ellipse in the horizontal plane. A minimum of three differently oriented common-midpoint (CMP) lines (or a "wide-azimuth" 3-D survey) is needed to reconstruct the ellipse and thus obtain NMO velocity in any azimuthal direction. Then, the orientation and the semiaxes of the NMO ellipse, which are dependent on both anisotropy and heterogeneity, can be inverted for the medium parameters.

Our analytic and numerical study shows that for the model of a homogeneous orthorhombic layer above a dipping reflector, the exact P-wave NMO velocity is determined by the symmetry-plane orientation and five parameters: the NMO velocities from a horizontal reflector measured in the symmetry planes $[V_{\rm nmo}^{(1,2)}]$ and three anisotropic coefficients $\eta^{(1,2,3)}$ introduced by analogy with the Alkhalifah-Tsvankin parameter η for VTI media. The importance of the medium parameterization in terms of the η coefficients goes well beyond the NMO-velocity function. By generating migration impulse responses, we demonstrate that the parameters $V_{\rm nmo}^{(1,2)}$ and $\eta^{(1,2,3)}$ are sufficient to perform all time processing steps (normal-moveout and dip-moveout corrections, prestack and poststack time migration) in orthorhombic models.

The velocities $V_{\rm nmo}^{(1,2)}$ and the orientation of the vertical symmetry planes can be found using the azimuthally dependent NMO velocity from a horizontal reflector. Then the NMO ellipse of at least one dipping event is additionally needed to obtain the coefficients $\eta^{(1,2,3)}$ that control the dip dependence of normal moveout. We discuss the stability of the inversion procedure and specify the constraints on the dip and azimuth of the reflector; for instance, for all three η coefficients to be resolved individually, the dip plane of the reflector should not coincide with either of the symmetry planes.

To carry out parameter estimation in vertically inhomogeneous orthorhombic media, we apply the generalized Dix equation of Grechka, Tsvankin and Cohen, which operates with the matrices responsible for interval NMO ellipses rather than with the NMO velocities themselves. Our algorithm is designed to find the interval values of $V_{\rm nmo}^{(1,2)}$ and $\eta^{(1,2,3)}$ using moveout from horizontal and dipping reflectors measured at different vertical times (i.e., only surface P-wave data are needed). Application to a synthetic multiazimuth P-wave data set over a layered orthorhombic medium with depth-varying orientation of the symmetry planes verifies the accuracy of the inversion method.

INTRODUCTION

Reflection moveout and, in particular, normal-moveout (NMO) velocity have been extensively used to build isotropic velocity models of the subsurface (e.g., Hubral and Krey, 1980). The main complication in extending these velocity-analysis methods to anisotropic media is the multiparameter nature of the problem: the angular dependence of the velocity function at each spatial location is described by several (up to 21) elastic coefficients. Even for relatively simple transversely isotropic (TI)

Presented at the 67th Annual International Meeting, Society of Exploration Geophysicists. Manuscript received by the Editor July 31, 1997; revised manuscript received August 26, 1998.
*Colorado School of Mines, Center for Wave Phenomena, Department of Geophysics, Golden, Colorado 80401. E-mail: vgrechka@dix.mines.edu; ilya@dix.mines.edu.

media, P- and SV-wave propagation (the qualifiers in "quasi–P-wave" and "quasi–S-wave" will be omitted) is governed by the orientation of the symmetry axis and four stiffness coefficients. This number, however, can be reduced if we focus exclusively on kinematic signatures of P-waves, which depend (for a fixed symmetry-axis orientation) on the symmetry-direction velocity V_{P0} and just two of Thomsen's anisotropic coefficients ϵ and δ (Tsvankin and Thomsen, 1994). Furthermore, as shown by Alkhalifah and Tsvankin (1995), P-wave NMO velocity and all time-processing steps [NMO and dip-moveout (DMO) correction, time migration] in TI models with a vertical symmetry axis (VTI media) are controlled by only two combinations of V_{P0}, ϵ, and δ: the zero-dip NMO velocity $V_{\rm nmo}(0)$ and the "anellipticity" coefficient $\eta \equiv (\epsilon - \delta)/(1 + 2\delta)$. Alkhalifah and Tsvankin (1995) also developed a method for obtaining $V_{\rm nmo}(0)$ and η in vertically inhomogeneous VTI media using P-wave NMO velocities from reflectors with two different dips (e.g., from horizontal and dipping interfaces). That algorithm, however, is based on the 2-D NMO equation of Tsvankin (1995), which can be applied only to common-midpoint (CMP) lines in the dip plane of the reflector.

Reflection moveout for out-of-plane (3-D) wave propagation in inhomogeneous anisotropic media was analyzed by Grechka and Tsvankin (1998b), who showed that the azimuthal dependence of NMO velocity is described by a simple quadratic form and typically represents an ellipse in the horizontal plane. In the special case of a horizontal layer with a horizontal symmetry plane, the elliptical dependence of NMO velocity was obtained by Sayers and Ebrom (1997), who developed an approximate representation of long-spread moveout based on an expansion of group velocity in spherical harmonics.

If the medium above a dipping reflector has the VTI symmetry, the axes of the NMO ellipse lie in the dip and strike directions of the reflector. Grechka and Tsvankin (1998b) proved that both semiaxes of the ellipse (and, therefore, the NMO velocity in any azimuthal direction) for P-waves in VTI media depend on just the two Alkhalifah-Tsvankin parameters, $V_{\rm nmo}(0)$ and η. NMO velocity and zero-offset traveltimes for a dipping event obtained on two CMP lines with different azimuthal orientation are needed to recover $V_{\rm nmo}(0)$ and η, along with the azimuth of the dip direction of the reflector. Alternatively, both parameters can be found using normal moveout from a horizontal and dipping reflector on a single CMP line with a known azimuthal orientation relative to the dip direction (Grechka and Tsvankin, 1998b). Additional azimuths, if available, provide redundant information that might increase the accuracy of the parameter estimation.

In this paper, we use the analytic results of Grechka and Tsvankin (1998b) and Grechka et al. (1999) to generalize this methodology for more complicated, azimuthally anisotropic media. The NMO ellipse for a given reflection event is always described by three independent parameters and can be reconstructed from NMO velocities measured in at least three different azimuthal directions. The feasibility of obtaining P-wave NMO ellipses in a "wide-azimuth" 3-D survey (one that has good offset coverage in a wide range of azimuthal angles) and using them for fracture detection has been shown by Corrigan et al. (1996) and Grechka et al. (1999).

The parameters of the NMO ellipse can be inverted for the combinations of the medium coefficients responsible for normal moveout of the P-wave or some other recorded mode. In general, this inversion requires moveout data for several reflectors with different dips and azimuths (depending on the symmetry of the medium). Although conceptually this problem can be solved for arbitrary anisotropic media, this work is restricted to orthorhombic (or orthotropic) anisotropy, which describes several models typical for fractured reservoirs (e.g., Wild and Crampin, 1991; Schoenberg and Helbig, 1997; Tsvankin, 1997). For instance, orthorhombic symmetry may be caused by a system of parallel vertical cracks embedded in a background VTI medium (Figure 1) and also by two orthogonal (or nonorthogonal but identical) vertical crack systems in a purely isotropic or VTI matrix. Although orthorhombic models with a fixed orientation of the symmetry planes are described by nine independent stiffnesses, P-wave velocities and traveltimes depend on just the vertical velocity and five anisotropic parameters introduced by Tsvankin (1997). Grechka and Tsvankin (1998b) provided exact explicit expressions for NMO velocity in a horizontal orthorhombic layer and demonstrated that Tsvankin's notation (briefly reviewed below) leads to a significant simplification in the analytic description of NMO velocity.

Extending this result to a homogeneous orthorhombic layer above a dipping reflector, we show that P-wave normal-moveout velocity (expressed through the horizontal slowness components of the zero-offset ray) depends on the orientation of the symmetry planes, symmetry-plane NMO velocities from a horizontal reflector [$V_{\rm nmo}^{(1,2)}$], and three anisotropic parameters $\eta^{(1,2,3)}$ defined similarly to the Alkhalifah-Tsvankin coefficient η. Furthermore, the same parameters are responsible for post-stack time-migration impulse response and, therefore, for all time-processing steps in orthorhombic media. This conclusion is in agreement with the work by Ikelle (1996), who showed that the dispersion relation in weakly anisotropic orthorhombic media depends on the two zero-dip NMO velocities in the symmetry planes and three "anellipticity" coefficients. All five parameters can be obtained from surface P-wave data using

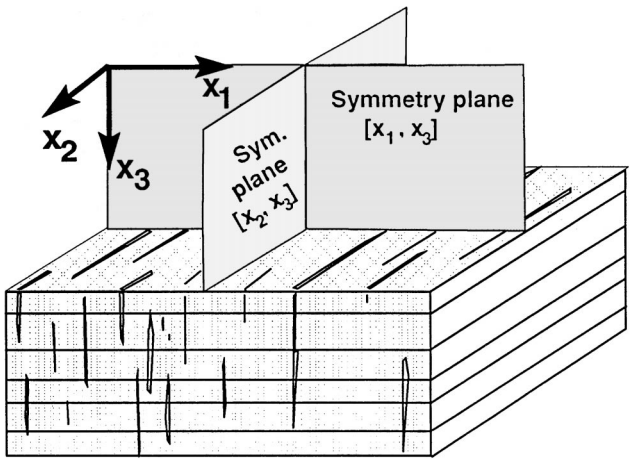

FIG. 1. Orthorhombic media have three mutually orthogonal planes of mirror symmetry. One of the models that would give rise to orthorhombic anisotropy is a combination of parallel vertical cracks and vertical transverse isotropy (e.g., due to thin horizontal layering) in the background medium.

azimuthally dependent NMO velocities from a horizontal and at least one dipping interface (provided the dip plane of the reflector is not too close to either of the vertical symmetry planes) or, alternatively, using two different dipping events. To find the interval values of $V_{\rm nmo}^{(1,2)}$ and $\eta^{(1,2,3)}$ in horizontally layered orthorhombic media above a dipping reflector, we devise a layer-stripping procedure based on the generalized Dix equation of Grechka et al. (1999). Finally, we apply our inversion algorithm to synthetic P-wave traveltimes generated by ray tracing for a stratified orthorhombic model with different orientations of the vertical symmetry planes in each layer.

NOTATION FOR ORTHORHOMBIC MEDIA

Orthorhombic (or orthotropic) media have three mutually orthogonal planes of mirror symmetry; for the model with a single system of vertical cracks in a VTI background (Figure 1), the symmetry planes are determined by the crack orientation. Here, we assume that one of the symmetry planes is horizontal, but we do not restrict ourselves to any particular physical model and consider a general stiffness tensor for orthorhombic media with nine independent components c_{ij}. Evidently, inverting moveout information for nine parameters (which can vary in space) is an extremely difficult problem, especially given a limited angle coverage of reflection data.

Significant progress, however, can be made by combining the stiffnesses in such a way that will simplify analytic descriptions of seismic velocities and amplitudes. Tsvankin (1997) used the fact that the Christoffel equation has the identical form in the symmetry planes of orthorhombic and TI media to introduce a notation based on the same principle as Thomsen (1986) parameters for vertical transverse isotropy. Tsvankin's notation contains two "isotropic" quantities (the vertical velocities of the P-wave and one of the split S-waves) and seven dimensionless anisotropic parameters similar to the VTI coefficients ϵ, δ, and γ. The definitions of these parameters and their brief description are as follows:

V_{P0}—the P-wave vertical velocity:

$$V_{P0} \equiv \sqrt{\frac{c_{33}}{\rho}}, \tag{1}$$

where ρ is the density.

V_{S0}—the vertical velocity of the S-wave polarized in the x_1-direction:

$$V_{S0} \equiv \sqrt{\frac{c_{55}}{\rho}}. \tag{2}$$

$\epsilon^{(2)}$—the VTI parameter ϵ in the $[x_1, x_3]$ symmetry plane normal to x_2-axis (this explains the superscript "2"):

$$\epsilon^{(2)} \equiv \frac{c_{11} - c_{33}}{2\,c_{33}}. \tag{3}$$

$\delta^{(2)}$—the VTI parameter δ in the $[x_1, x_3]$ plane:

$$\delta^{(2)} \equiv \frac{(c_{13} + c_{55})^2 - (c_{33} - c_{55})^2}{2\,c_{33}\,(c_{33} - c_{55})}. \tag{4}$$

$\gamma^{(2)}$—the VTI parameter γ in the $[x_1, x_3]$ plane:

$$\gamma^{(2)} \equiv \frac{c_{66} - c_{44}}{2c_{44}}. \tag{5}$$

$\epsilon^{(1)}$—the VTI parameter ϵ in the $[x_2, x_3]$ symmetry plane:

$$\epsilon^{(1)} \equiv \frac{c_{22} - c_{33}}{2c_{33}}. \tag{6}$$

$\delta^{(1)}$—the VTI parameter δ in the $[x_2, x_3]$ plane:

$$\delta^{(1)} \equiv \frac{(c_{23} + c_{44})^2 - (c_{33} - c_{44})^2}{2c_{33}(c_{33} - c_{44})}. \tag{7}$$

$\gamma^{(1)}$—the VTI parameter γ in the $[x_2, x_3]$ plane:

$$\gamma^{(1)} \equiv \frac{c_{66} - c_{55}}{2\,c_{55}}. \tag{8}$$

$\delta^{(3)}$—the VTI parameter δ in the $[x_1, x_2]$ plane (x_1 plays the role of the symmetry axis):

$$\delta^{(3)} \equiv \frac{(c_{12} + c_{66})^2 - (c_{11} - c_{66})^2}{2\,c_{11}\,(c_{11} - c_{66})}. \tag{9}$$

This notation preserves the attractive features of Thomsen parameters (discussed in detail by Tsvankin, 1996) in describing symmetry-plane velocities, traveltimes, and reflection coefficients. Also, as shown in Tsvankin (1997), a subset of the parameters introduced above captures the combinations of c_{ij}'s responsible for P-wave kinematic signatures both within and outside symmetry planes, even for strongly anisotropic orthorhombic media. P-wave velocities and traveltimes (including reflection moveout) depend on just six parameters (V_{P0}, $\epsilon^{(1)}$, $\delta^{(1)}$, $\epsilon^{(2)}$, $\delta^{(2)}$, and $\delta^{(3)}$) and the orientation of the symmetry planes, rather than nine coefficients in the conventional (c_{ij}) notation. Since the parameters $\delta^{(1)}$ and $\delta^{(2)}$ determine near-vertical P-wave velocity variations, they concisely describe P-wave NMO velocity from horizontal reflectors (Grechka and Tsvankin, 1998b). The results below show that normal moveout of dipping events is a function of simple combinations of ϵ's and δ's as well.

Another advantage of this notation is the convenience of characterizing anisotropy by a set of dimensionless anisotropic coefficients that go to zero in isotropic media and are well suited for developing weak-anisotropy approximations for various seismic signatures. Below, we apply the weak-anisotropy approximation to the NMO-velocity function to identify the parameters that govern P-wave moveout in orthorhombic media.

EQUATION OF THE NMO ELLIPSE

Grechka and Tsvankin (1998b) considered azimuthally dependent reflection moveout of pure (nonconverted) modes around a certain CMP location over an arbitrary anisotropic heterogeneous medium. By expanding the one-way traveltime τ from the zero-offset reflection point to the surface into a double Taylor series with respect to the horizontal Cartesian coordinates (x_1, x_2), they derived the following expression for the normal-moveout velocity (see also Grechka et al., 1999):

$$V_{\rm nmo}^{-2}(\alpha) = W_{11}\cos^2\alpha + 2\,W_{12}\sin\alpha\cos\alpha + W_{22}\sin^2\alpha\,, \tag{10}$$

where α is the azimuth of the CMP line with respect to the x_1-axis, and the symmetric matrix $\mathbf{W}$ is given by

$$W_{ij} = \tau_0\,\frac{\partial^2\tau}{\partial x_i\,\partial x_j}\bigg|_{\tau=\tau_0} = \tau_0\,\frac{\partial p_i}{\partial x_j}, \qquad (i, j = 1, 2). \tag{11}$$

Here, τ_0 is the one-way zero-offset traveltime, and p_1 and p_2 are the horizontal components of the slowness vector; the spatial derivatives of τ and p_i are evaluated for the zero-offset ray (i.e., at the CMP location). Grechka and Tsvankin (1998b) showed that if the CMP traveltime increases with offset for all azimuths α (which is usually the case), the matrix $\mathbf{W}$ is positive definite, and the azimuthally varying NMO velocity (10) represents an ellipse. To demonstrate the elliptical character of $V_{\rm nmo}(\alpha)$, equation (10) can be rewritten as (for details, see Grechka and Tsvankin, 1998b; Grechka et al., 1999)

$$V_{\rm nmo}^{-2}(\alpha) = \lambda_1 \cos^2(\alpha - \beta) + \lambda_2 \sin^2(\alpha - \beta), \qquad (12)$$

where $\lambda_{1,2}$ are the eigenvalues of the matrix $\mathbf{W}$, and β is the rotation angle (determined by the eigenvectors of $\mathbf{W}$) defined as

$$\beta = \tan^{-1}\left[\frac{W_{22} - W_{11} + \sqrt{(W_{22} - W_{11})^2 + 4W_{12}^2}}{2W_{12}}\right]. \qquad (13)$$

Except for uncommon models with reverse moveout (i.e., with negative $V_{\rm nmo}^2$, which implies that $\lambda_1 < 0$ and/or $\lambda_2 < 0$), equation (12) does indeed describe an ellipse in the horizontal plane. The NMO velocities in the directions of the elliptical axes (we denote them $V_{e\ell 1}$ and $V_{e\ell 2}$) are expressed through the eigenvalues as $V_{e\ell 1} = 1/\sqrt{\lambda_1}$ and $V_{e\ell 2} = 1/\sqrt{\lambda_2}$.

Since the NMO ellipse (10) is fully defined by only three quantities (W_{11}, W_{12}, and W_{22}), it can be reconstructed from reflection data using a minimum of three NMO-velocity measurements in different azimuthal directions. Below, we show how the elements of the matrix $\mathbf{W}$ for horizontal and dipping events can be inverted for the parameters of orthorhombic media.

NMO VELOCITY IN A HOMOGENEOUS ORTHORHOMBIC LAYER

Horizontal layer

As mentioned above, we consider an orthorhombic medium with a horizontal symmetry plane. Then the azimuths of the other two (vertical) symmetry planes determine the orientation of the NMO ellipse in a horizontal orthorhombic layer, which can be demonstrated by aligning the coordinate directions x_1 and x_2 with the vertical symmetry planes. In this case, $W_{12} = 0$, and equation (10) reduces to (Grechka and Tsvankin, 1998b)

$$\begin{aligned} V_{\rm nmo}^{-2}(\alpha, 0) &= W_{11}\cos^2\alpha + W_{22}\sin^2\alpha \\ &= \left[V_{\rm nmo}^{(2)}\right]^{-2}\cos^2\alpha + \left[V_{\rm nmo}^{(1)}\right]^{-2}\sin^2\alpha, \end{aligned} \qquad (14)$$

where $V_{\rm nmo}^{(2)}$ and $V_{\rm nmo}^{(1)}$ are the NMO velocities in the symmetry planes $[x_1, x_3]$ and $[x_2, x_3]$, respectively, which can be easily found by analogy with vertical transverse isotropy (Tsvankin, 1997). For instance, the symmetry-plane NMO velocities for P-waves are given by

$$V_{\rm nmo}^{(i)} = V_{P0}\sqrt{1 + 2\delta^{(i)}}, \qquad (i = 1, 2), \qquad (15)$$

where V_{P0} and $\delta^{(i)}$ are introduced in equations (1), (4), and (7). The remarkable simplicity of the exact NMO equations (14) and (15) illustrates the advantages of Tsvankin's parameterization (1)–(9).

Clearly, by obtaining the P-wave NMO ellipse in a horizontal orthorhombic layer, we can determine the orientation of the vertical symmetry planes and the NMO velocities $V_{\rm nmo}^{(1,2)}$ within them. The only case in which the azimuths of the symmetry planes cannot be resolved is when the ellipse degenerates into a circle (i.e., $V_{\rm nmo}^{(2)} = V_{\rm nmo}^{(1)}$). Likewise, the symmetry-plane directions can be recovered from the azimuthally dependent NMO velocities of either split shear mode.

Layer above a dipping reflector

NMO equation for general anisotropy.—If the bottom of a homogeneous orthorhombic layer is dipping, the azimuthal dependence of NMO velocity is influenced by both the reflector orientation and azimuthal anisotropy. Unless the dip plane of the reflector coincides with one of the symmetry planes of the medium, the model as a whole no longer has vertical symmetry planes, and NMO velocity cannot be described by equation (14). Whereas the azimuthal variation of normal-moveout velocity remains elliptical in accordance with the general equation (10), the semiaxes of the NMO ellipse do not necessarily coincide with the symmetry-plane directions of the layer above the reflector.

For the purposes of traveltime inversion, it is essential to express the NMO velocity through quantities that can be measured from reflection data. In the 2-D problem dealing with moveout in the dip plane of the reflector (which should coincide with a symmetry plane of the medium), the slope of reflections on the zero-offset section yields the ray parameter (horizontal slowness) of the zero-offset ray (Alkhalifah and Tsvankin, 1995). (In contrast, recovering the actual dip of the reflector from reflection traveltimes requires knowledge of the velocity field, even if the medium is purely isotropic.)

Similarly, in the more general 3-D case discussed here, the horizontal components (p_1 and p_2) of the zero-offset slowness vector can be obtained directly from the azimuthally dependent slope of zero-offset reflections. Although we do need a minimum of three different azimuths to reconstruct the NMO ellipse, the zero-offset sections along any two of them can be used to find p_1 and p_2 (Grechka and Tsvankin, 1998b). Indeed, the zero-offset reflection slope in any azimuthal direction is simply equal to the projection of the zero-offset slowness vector onto this direction. Snell's law implies that the slowness vector of the zero-offset ray (but not necessarily the ray itself) is normal to the reflector at the zero-offset reflection point. The components p_1 and p_2, therefore, allow us to determine reflector azimuth, while the dip still remains unknown because the vertical slowness component cannot be found directly from traveltimes measured in the horizontal plane.

The analysis below is based on the exact explicit expession for NMO velocity in a homogeneous layer of arbitrary symmetry given by Grechka et al. (1999), who expressed the components of the matrix $\mathbf{W}$ through the slowness vector of the zero-offset ray as

$$\mathbf{W} = \frac{p_1 q_{,1} + p_2 q_{,2} - q}{q_{,11}q_{,22} - q_{,12}^2}\begin{pmatrix} q_{,22} & -q_{,12} \\ -q_{,12} & q_{,11} \end{pmatrix}, \qquad (16)$$

where $q \equiv q(p_1, p_2) \equiv p_3$ is the vertical component of the slowness vector; $q_{,i}$ and $q_{,ij}$, $(i, j = 1, 2)$ denote the partial

derivatives $q_{,i} \equiv \partial q/\partial p_i$ and $q_{,ij} \equiv \partial^2 q/\partial p_i \partial p_j$ that should be evaluated for the zero-offset ray. Substitution of **W** into equation (10) for the NMO ellipse yields

$$V_{\rm nmo}^{-2}(\alpha, p_1, p_2) = \frac{p_1 q_{,1} + p_2 q_{,2} - q}{q_{,11} q_{,22} - q_{,12}^2} \times \left[q_{,22}\cos^2\alpha - 2q_{,12}\sin\alpha\cos\alpha + q_{,11}\sin^2\alpha\right]. \tag{17}$$

Equation (17) is valid for all pure (i.e., nonconverted) reflection modes and any mutual orientation of the CMP line and reflector strike. The vertical slowness $q \equiv p_3$ can be found from the Christoffel equation,

$$\det(c_{ijkl}\, p_j\, p_k - \rho\delta_{il}) = 0, \tag{18}$$

where δ_{il} is the Kronecker's symbolic delta. Note that in a medium with a horizontal symmetry plane (the case considered here), the Christoffel equation reduces to a cubic polynomial with respect to q^2. The derivatives $q_{,i}$ and $q_{,ij}$ can be calculated by implicit differentiation of equation (18), as described by Grechka et al. (1999).

Although the NMO equation (17) is quite general, here we apply it only to P-waves in orthorhombic media. Since the NMO ellipse (17) is defined by three components of the matrix **W** (i.e., three coefficients of the trigonometric functions), no more than three combinations of the layer parameters can be extracted from moveout measurements for a single reflector with certain values of p_1 and p_2. As discussed above, if the reflector is horizontal, P-wave NMO velocity is sufficient to determine the orientation of the symmetry planes and the NMO velocities within them. An important question addressed below is which parameters of an orthorhombic medium can be obtained using P-wave NMO velocity from dipping reflectors with different strike orientations.

***P*-wave NMO velocity in the weak-anisotropy limit.**—Although numerical evaluation of equation (17) is relatively straightforward, the dependence of NMO velocity on the medium parameters is hidden in the slowness components and their derivatives. Therefore, to identify the coefficients responsible for P-wave NMO velocity, it is convenient to apply the weak-anisotropy approximation. This approach has proved extremely productive in the analysis of NMO velocity and other seismic signatures for vertical transverse isotropy (Tsvankin, 1995, 1996; Alkhalifah and Tsvankin, 1995; Cohen, 1997). For instance, Alkhalifah and Tsvankin (1995) provided analytic support for their two-parameter methodology by showing that P-wave NMO velocity in weakly anisotropic VTI media depends just on the zero-dip value $V_{\rm nmo}(0)$ and the difference $\epsilon - \delta \approx \eta$. Cohen (1997) further substantiated this conclusion by analyzing the weak-anisotropy approximation quadratic in the anisotropic parameters.

To express the vertical slowness through p_1 and p_2, we use the P-wave phase-velocity equation for weakly orthorhombic media given in Tsvankin (1997):

$$V^2 = V_{P0}^2\big[1 + 2n_1^4\epsilon^{(2)} + 2n_2^4\epsilon^{(1)} + 2n_1^2n_3^2\delta^{(2)} + 2n_2^2n_3^2\delta^{(1)} + 2n_1^2n_2^2(2\epsilon^{(2)} + \delta^{(3)})\big]. \tag{19}$$

Here $\mathbf{n} = \mathbf{p}V$ is the unit vector parallel to the slowness vector **p** defined in the coordinate system associated with the symmetry planes (i.e., $[x_1, x_3]$ is a vertical symmetry plane), V_{P0} is the vertical P-wave velocity [equation (1)], and $\epsilon^{(i)}$ and $\delta^{(i)}$ are Tsvankin's anisotropic parameters [equations (3), (4), (6), (7), and (9)]. Equation (19) is fully linearized in the dimensionless anisotropic coefficients that are supposed to be small in the limit of weak anisotropy.

Substituting the slowness vector **p** into equation (19), we obtain the vertical slowness $q \equiv p_3$ as an explicit function of the horizontal slowness components.

$$q^2 = \left(\frac{1}{V_{P0}^2} - p_1^2 - p_2^2\right) - 2V_{P0}^2\left\{\left(p_1^2 + p_2^2\right) \times \left[p_1^2(\epsilon^{(2)} - \delta^{(2)}) + p_2^2(\epsilon^{(1)} - \delta^{(1)})\right] + \frac{p_1^2\delta^{(2)} + p_2^2\delta^{(1)}}{V_{P0}^2} + p_1^2p_2^2\left(\epsilon^{(1)} - \epsilon^{(2)} - \delta^{(3)}\right)\right\}. \tag{20}$$

As follows from equations (19) and (20), in the weak anisotropy approximation both the P-wave phase velocity V and the vertical component of the slowness vector q depend on only six quantities: the vertical velocity V_{P0} and five anisotropic parameters $\epsilon^{(1)}$, $\epsilon^{(2)}$, $\delta^{(1)}$, $\delta^{(2)}$, and $\delta^{(3)}$. Since phase velocity determines all other kinematic signatures of a given mode, these six parameters fully control P-wave velocities and traveltimes in weakly orthorhombic media. Tsvankin (1997) proved that this conclusion remains valid even for strong velocity anisotropy when the weak-anisotropy equations become numerically inaccurate.

It is also important to recognize that equation (20) contains the combinations $\epsilon^{(2)} - \delta^{(2)}$ and $\epsilon^{(1)} - \delta^{(1)}$, which represent the linearized versions of the "anellipticity" coefficients $\eta^{(2)}$ and $\eta^{(1)}$ introduced in Tsvankin (1997) by analogy with the Alkhalifah-Tsvankin coefficient η:

$\eta^{(2)}$—the VTI parameter η in the vertical symmetry plane $[x_1, x_3]$:

$$\eta^{(2)} \equiv \frac{\epsilon^{(2)} - \delta^{(2)}}{1 + 2\,\delta^{(2)}}. \tag{21}$$

$\eta^{(1)}$—the VTI parameter η in the vertical symmetry plane $[x_2, x_3]$:

$$\eta^{(1)} \equiv \frac{\epsilon^{(1)} - \delta^{(1)}}{1 + 2\,\delta^{(1)}}. \tag{22}$$

In the linearized weak-anisotropy approximation, $\eta^{(2)} \approx \epsilon^{(2)} - \delta^{(2)}$ and $\eta^{(1)} \approx \epsilon^{(1)} - \delta^{(1)}$.

The kinematic equivalence between the symmetry planes of orthorhombic and VTI media implies that $\eta^{(2)}$ and $\eta^{(1)}$ are responsible for the "2-D" P-wave NMO-velocity function in the $[x_1, x_3]$ and $[x_2, x_3]$ planes, respectively. This equivalence, however, is valid only if the symmetry plane coincides with the dip plane of the reflector; otherwise, reflected rays propagate outside the vertical incidence plane and are influenced by azimuthal velocity variations.

Equation (20) also contains a linear combination of the anisotropic coefficients $(\epsilon^{(1)} - \epsilon^{(2)} - \delta^{(3)})$ that involves the parameter $\delta^{(3)}$ specified for the horizontal symmetry plane $[x_1, x_2]$

[equation (9)]. To identify this combination as another linearized η coefficient, this time corresponding to the $[x_1, x_2]$ plane, let us recall the definition of η for VTI media (Alkhalifah and Tsvankin, 1995):

$$\eta \equiv \frac{1}{2}\left[\frac{V_{\rm hor}^2}{V_{\rm nmo}^2(0)} - 1\right]. \tag{23}$$

In applying equation (23) to the $[x_1, x_2]$ symmetry plane, we have to keep in mind that x_1 plays the role of the symmetry axis of the equivalent VTI medium [see equation (9)]. Hence, the horizontal velocity should be evaluated in the x_2-direction:

$$V_{\rm hor} = V_{\rm nmo}^{(1)}\sqrt{1+2\eta^{(1)}} = V_{P0}\sqrt{1+2\epsilon^{(1)}},$$

whereas the corresponding "$V_{\rm nmo}(0)$" is given by

$$\begin{aligned} V_{\rm nmo}(0) &= V_{\rm nmo}^{(2)}\sqrt{1+2\eta^{(2)}}\,\sqrt{1+2\delta^{(3)}} \\ &= V_{P0}\sqrt{1+2\epsilon^{(2)}}\,\sqrt{1+2\delta^{(3)}}. \end{aligned}$$

Substituting these values of $V_{\rm hor}$ and $V_{\rm nmo}(0)$ into equation (23), we define the η coefficient in the $[x_1, x_2]$ plane as

$$\begin{aligned} \eta^{(3)} &\equiv \frac{1}{2}\left\{\frac{\left[V_{\rm nmo}^{(1)}\right]^2(1+2\eta^{(1)})}{\left[V_{\rm nmo}^{(2)}\right]^2(1+2\eta^{(2)})(1+2\delta^{(3)})} - 1\right\} \\ &= \frac{\epsilon^{(1)} - \epsilon^{(2)} - \delta^{(3)}(1+2\epsilon^{(2)})}{(1+2\epsilon^{(2)})(1+2\delta^{(3)})}. \end{aligned} \tag{24}$$

For weak orthorhombic anisotropy, $\eta^{(3)}$ reduces to the linear combination $(\epsilon^{(1)} - \epsilon^{(2)} - \delta^{(3)})$ from equation (20). The expression for $\eta^{(3)}$ is more complicated than those for $\eta^{(1)}$ and $\eta^{(2)}$ because neither the velocity along the x_1-axis (the symmetry axis of the effective VTI medium) nor the coefficient ϵ in the $[x_1, x_2]$ plane are included in Tsvankin's parameterization (both would be redundant).

Introducing the values of $\eta^{(1)}$, $\eta^{(2)}$, and $\eta^{(3)}$ into the expression for the vertical slowness q [equation (20)], substituting q and its derivatives into the NMO equation (17) and carrying out further linearization in the anisotropic coefficients, we find the following weak-anisotropy approximation for P-wave NMO velocity (Appendix A):

$$\begin{aligned} V_{\rm nmo}^{-2}(\alpha, p_1, p_2) &= \cos^2\alpha\left\{\left[V_{\rm nmo}^{(2)}\right]^{-2} - p_1^2 + \sum_{i=1}^{3} d_{1i}\,\eta^{(i)}\right\} \\ &+ 2\sin\alpha\cos\alpha\left\{-p_1 p_2 + \sum_{i=1}^{3} d_{2i}\,\eta^{(i)}\right\} \\ &+ \sin^2\alpha\left\{\left[V_{\rm nmo}^{(1)}\right]^{-2} - p_2^2 + \sum_{i=1}^{3} d_{3i}\,\eta^{(i)}\right\}, \end{aligned} \tag{25}$$

where $V_{\rm nmo}^{(1,2)}$ [equations (A-12)] are the linearized symmetry-plane NMO velocities from a horizontal reflector (i.e., the semiaxes of the corresponding NMO ellipse), $\eta^{(i)}$ are the linearized versions of the parameters defined in equations (21), (22), and (24), and the quantities $d_{ki}(p_1, p_2)$ are given in Appendix A. The azimuth α in equation (25) is measured from the $[x_1, x_3]$ symmetry plane. Note that for a horizontal reflector $p_1 = p_2 = d_{ki} = 0$, and equation (25) reduces to the NMO ellipse for a horizontal orthorhombic layer given by equation (14).

Although, as discussed above, P-wave phase velocity depends on six medium parameters, only five combinations of them ($V_{\rm nmo}^{(1)}$, $V_{\rm nmo}^{(2)}$, $\eta^{(1)}$, $\eta^{(2)}$, and $\eta^{(3)}$) determine the P-wave NMO velocity (25) in the weak anisotropy limit. This indicates that the NMO ellipse (25) for a dipping reflector ($p_1 \neq 0$ and/or $p_2 \neq 0$) can be inverted for the three η coefficients provided $V_{\rm nmo}^{(1)}$, $V_{\rm nmo}^{(2)}$, and the orientation of the vertical symmetry planes have already been found using horizontal events.

To gain analytic insight into the possibility of recovering all three η coefficients from a single dipping event, let us assume that the dip azimuth of the reflector is aligned with one of the vertical symmetry planes. We will show that in this case the inversion can yield only one η coefficient and the difference between the two others.

Suppose, for instance, that the dip azimuth coincides with the x_1-direction. Then, the zero-offset slowness vector (and the zero-offset ray) is confined to the $[x_1, x_3]$ symmetry plane, and the horizontal slowness component p_2 is equal to zero. Evaluating the coefficients d_{ki} [equations (A-2)–(A-10)] for $p_2 = 0$ and substituting the results into the NMO equation (25), we obtain

$$\begin{aligned} &V_{\rm nmo}^{-2}(\alpha, p_1, p_2 = 0) = \\ &\quad\cos^2\alpha\left\{\left[V_{\rm nmo}^{(2)}\right]^{-2} - p_1^2 - 2p_1^2\eta^{(2)}\left(4p_1^4\tilde{V}^4 - 9p_1^2\tilde{V}^2 + 6\right)\right\} \\ &\quad+ \sin^2\alpha\left\{\left[V_{\rm nmo}^{(1)}\right]^{-2} - 2p_1^2\left[\eta^{(1)} - \eta^{(3)} + \eta^{(2)}\left(1 - p_1^2\tilde{V}^2\right)\right]\right\}, \end{aligned} \tag{26}$$

where $\tilde{V} = \frac{1}{2}(V_{\rm nmo}^{(1)} + V_{\rm nmo}^{(2)})$; as discussed in Appendix A, in the linearized weak-anisotropy approximation, it is possible to add any anisotropic terms to $\tilde{V}$ without changing the final expression. Equation (26) shows that the semiaxes of the NMO ellipse are parallel to the dip and strike directions of the reflector. This result (which is valid for any strength of the anisotropy, see Grechka and Tsvankin, 1998b; Grechka et al., 1999) could be expected because the dip plane becomes a plane of symmetry for the whole model.

If the azimuths of the symmetry planes have already been found from horizontal events, the orientation of the ellipse does not carry new information about anisotropy. Therefore, in this case, the NMO ellipse for a single dipping event can be used to recover only two combinations of the medium parameters contained in the elliptical semiaxes. According to equation (26), the NMO velocity in the dip plane of the reflector ($\alpha = 0$) is given by

$$\begin{aligned} &V_{\rm nmo}^{-2}(0, p_1) = \\ &\quad\left[V_{\rm nmo}^{(2)}\right]^{-2} - p_1^2 - 2p_1^2\eta^{(2)} \times \left(4p_1^4\tilde{V}^4 - 9p_1^2\tilde{V}^2 + 6\right), \end{aligned} \tag{27}$$

which reduces to the weak-anisotropy approximation for the dip-line P-wave NMO velocity in VTI media derived by Alkhalifah and Tsvankin (1995) [their equation (A-10)], if we choose $\tilde{V}$ as $V_{\rm nmo}^{(2)}$ and recall that $\eta^{(2)}$ and $V_{\rm nmo}^{(2)}$ are equivalent to the VTI parameters η and $V_{\rm nmo}(0)$. Since the reflected rays on the dip line cannot deviate from the incidence (symmetry) plane, $V_{\rm nmo}(0, p_1)$ should indeed be given by the VTI equation (for any strength of the anisotropy) due to the kinematic

analogy between the symmetry planes of orthorhombic and VTI media (Tsvankin, 1997). Conclusions of Alkhalifah and Tsvankin (1995) drawn for VTI media imply that the NMO velocity in the $[x_1, x_3]$ plane can be inverted in a stable fashion for the coefficient $\eta^{(2)}$, if the reflector dip (represented by the horizontal slowness p_1) reaches at least 20–25°.

Additional information about the medium parameters is contained in the NMO velocity $V_{\rm nmo}(\pi/2, p_1)$ measured in the strike direction (the second semiaxis of the NMO ellipse). Equation (26) indicates that $V_{\rm nmo}(\pi/2, p_1)$ depends on the difference $\eta^{(1)} - \eta^{(3)}$ rather than on the individual values of $\eta^{(1)}$ and $\eta^{(3)}$. Therefore, if the $[x_1, x_3]$ plane is orthogonal to the strike of a dipping reflector, the semiaxes of the NMO ellipse can be inverted for the parameter $\eta^{(2)}$ and the difference $\eta^{(1)} - \eta^{(3)}$ (the NMO velocities from a horizontal reflector are assumed to be known). Likewise, if the reflector strike is normal to the $[x_2, x_3]$ plane, we can expect to obtain $\eta^{(1)}$ and the difference $\eta^{(2)} - \eta^{(3)}$. (Note that in the weak-anisotropy approximation, the definition of $\eta^{(3)}$ is symmetric in the sense that it does not change if we use x_2 as the symmetry axis of the effective VTI medium in the $[x_1, x_2]$ plane.) Therefore, resolving all three η coefficients individually requires the presence of a dipping reflector with the strike that deviates sufficiently from both vertical symmetry planes.

As shown in Appendix A, the VTI equation (27) can be used on the dip line even outside the symmetry planes, but with the azimuthally dependent zero-dip NMO velocity and η coefficient. This result, valid only for weak anisotropy, follows from the identical form of the phase-velocity equation in any vertical plane of orthorhombic and VTI media (Tsvankin, 1997). A more detailed discussion of the equivalence between VTI and orthorhombic media for out-of-plane propagation can be found in Rommel and Tsvankin (1997).

***P*-wave NMO velocity for strong anisotropy.**—The main purpose of applying the weak-anisotropy approximation to the NMO equation was to gain insight into the dependence of the moveout function on the anisotropy parameters. In the actual inversion procedure described below, we use the exact equation (17) valid for any strength of the anisotropy. Therefore, it is necessary to find out whether the parameters $V_{\rm nmo}^{(1)}$, $V_{\rm nmo}^{(2)}$, $\eta^{(1)}$, $\eta^{(2)}$, and $\eta^{(3)}$ alone control the P-wave NMO velocity for models with strong velocity variations. It should be emphasized that here and below we use the definitions of the η coefficients given in equations (21), (22), and (23) rather than their linearized weak-anisotropy approximations.

If the dip plane of the reflector coincides with one of the vertical symmetry planes, the dip-line NMO velocity is given by the VTI equations and, therefore, is fully determined by the zero-dip NMO velocity (i.e., the velocity from a horizontal reflector) and the corresponding η coefficient (Tsvankin, 1997). Even in this special case, however, the strike-line NMO velocity is influenced by azimuthal velocity variations and has to be studied separately.

To show that the five parameters listed above are indeed sufficient to describe the 3-D P-wave NMO velocity for strongly anisotropic media, we performed several numerical tests. A typical result for a reflector with the dip-plane azimuth diverging by 30° from the $[x_1, x_3]$ symmetry plane is displayed in Figure 2. The NMO ellipse, explicitly defined in equation (12), was characterized by its semiaxes $V_{e\ell 1}$ and $V_{e\ell 2}$ (Figures 2a,b) and the rotation angle β between the larger semiaxis and the $[x_1, x_3]$ symmetry plane (Figure 2c). All three parameters were calculated for a wide range of reflector dips governed by the horizontal slowness $p = \sqrt{p_1^2 + p_2^2}$. In the first test, we varied the ϵ and δ coefficients keeping the parameters $V_{\rm nmo}^{(1)}$, $V_{\rm nmo}^{(2)}$, $\eta^{(1)}$, $\eta^{(2)}$, and $\eta^{(3)}$ constant (compare the solid and dashed lines). Clearly, the NMO ellipses for these significantly different strongly anisotropic models, which have the same parameters $V_{\rm nmo}^{(1,2)}$ and $\eta^{(1,2,3)}$, practically coincide for all dips. In

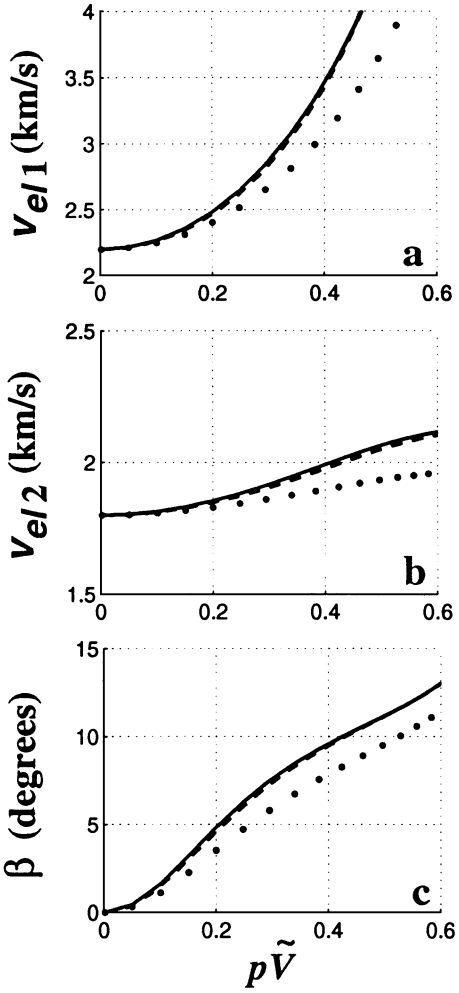

FIG. 2. The dependence of the NMO ellipse for reflections from a dipping interface on the parameters of an orthorhombic layer. The dip plane of the reflector makes an angle of 30° with the $[x_1, x_3]$ symmetry plane; the reflector dip changes in accordance with the horizontal slowness (ray parameter) $p = \sqrt{p_1^2 + p_2^2}$. (a) and (b) P-wave NMO velocities in the directions of the semiaxes of the NMO ellipse; (c) the rotation angle β of the larger semiaxis with respect to the $[x_1, x_3]$–plane. Solid line (model 1): $V_{\rm nmo}^{(1)} = 1.8$ km/s, $V_{\rm nmo}^{(2)} = 2.2$ km/s, $\eta^{(1)} = 0.2$, $\eta^{(2)} = 0.3$, $\eta^{(3)} = 0.15$, $\epsilon^{(1)} = 0.2$, $\epsilon^{(2)} = 0.695$, $\delta^{(1)} = 0$, $\delta^{(2)} = 0.25$, $\delta^{(3)} = -0.27$. Dashed line (model 2): all $V_{\rm nmo}^{(i)}$ and $\eta^{(i)}$ are the same as above, but $\epsilon^{(1)} = -0.031$, $\epsilon^{(2)} = 0.3$, $\delta^{(1)} = -0.165$, $\delta^{(2)} = 0$, $\delta^{(3)} = -0.27$. Dotted line (model 3): $V_{\rm nmo}^{(1)} = 1.8$ km/s, $V_{\rm nmo}^{(2)} = 2.2$ km/s, $\eta^{(1)} = 0.1$, $\eta^{(2)} = 0.2$, $\eta^{(3)} = 0.15$. $\tilde{V}$ is defined by equation (A-11).

contrast, variation in the relevant parameter combinations $\eta^{(1)}$ and $\eta^{(2)}$ (dotted) leads to noticeable changes in the semiaxes and orientation of the NMO ellipse with increasing dip. The substantial magnitude of the influence of $\eta^{(1)}$ and $\eta^{(2)}$ on normal moveout indicates that these coefficients can be obtained in a stable fashion from the NMO ellipse for a dipping event (provided the dip is not too mild).

Similar results have been obtained for a wide range of reflector azimuths and the values of anisotropic parameters. Thus, for a fixed orientation of the vertical symmetry planes, the exact NMO velocity $V_{\rm nmo}(\alpha, p_1, p_2)$ is a function of only five medium parameters: $V_{\rm nmo}^{(1,2)}$ and $\eta^{(1,2,3)}$. From equation (24), it is clear that $\eta^{(3)}$ can be replaced by the original coefficient $\delta^{(3)}$ of Tsvankin (1997), but we prefer to use $\eta^{(3)}$ to maintain uniformity in the definition of the coefficients. Also, $\eta^{(3)}$ appears to be a more natural choice for the moveout-inversion problem because it directly enters the weak-anisotropy approximation for the vertical slowness [equation (20)].

To recover these five parameters along with the symmetry-plane azimuths, we need a minimum of six moveout measurements which, in principle, can be obtained from at least two NMO ellipses corresponding to two distinct reflector dips and/or azimuths. In terms of the acquisition design, we need good offset coverage in at least three different azimuthal directions to reconstruct the elliptical NMO-velocity dependencies and determine the horizontal slowness components of the corresponding reflection events.

INVERSION OF *P*-WAVE NMO VELOCITY IN A SINGLE LAYER

Although in principle the inverse problem can be posed for two arbitrary reflector dips, for the sake of simplicity we assume that one of the reflectors is horizontal. The NMO ellipse for the horizontal event [equation (14)] provides the azimuths of the symmetry planes and the NMO velocities $V_{\rm nmo}^{(1,2)}$ within them. Then the zero-offset traveltimes of the dipping reflection, measured in different azimuthal directions, can be used to find the horizontal slowness components p_1 and p_2 of the zero-offset ray, while the corresponding NMO ellipse can be inverted for the parameters $\eta^{(1,2,3)}$. We formulate the conditions necessary for resolving all three η coefficients and study the stability of the inversion procedure in the presence of errors in input data.

This algorithm relies on the difference between the symmetry-plane NMO velocities for reflections from a horizontal interface to find the orientation of the symmetry planes. It may happen, however, that $V_{\rm nmo}^{(1)} = V_{\rm nmo}^{(2)}$ ($\delta^{(1)} = \delta^{(2)}$), and the NMO ellipse for horizontal events degenerates into a circle. In this case (not discussed here), we need two different dipping events to recover the symmetry-plane azimuths and the three η coefficients.

If $V_{\rm nmo}^{(1,2)}$ and the orientation of the symmetry planes have been obtained, the elements of the matrix $\mathbf{W}$ for a dipping event with the horizontal slowness components p_1 and p_2 become functions of $\eta^{(1,2,3)}$ [see equation (16)]:

$$W_{ij}\left(\eta^{(1)}, \eta^{(2)}, \eta^{(3)}\right) = q_{,ij}(2\delta_{ij} - 1) \times \frac{p_1 q_{,1} + p_2 q_{,2} - q}{q_{,11} q_{,22} - q_{,12}^2}, \qquad (i, j = 1, 2), \tag{28}$$

where δ_{ij} is the Kronecker's δ. Since the matrix $\mathbf{W}$ is symmetric, the system (28) contains three nonlinear equations for the three unknowns. We obtain the η coefficients by using the simplex method to solve the following least-squares problem:

$$\mathcal{F}_P \equiv \sum_{i,j=1}^{2} \left[\hat{W}_{ij} - W_{ij}\left(\eta^{(1)}, \eta^{(2)}, \eta^{(3)}\right)\right]^2 = \min, \tag{29}$$

where $\hat{\mathbf{W}}$ is the matrix that determines the NMO ellipse reconstructed from azimuthally dependent moveout data. Numerical tests (see examples below) performed with various initial guesses showed that the inversion algorithm successfully converges towards the correct values of $\eta^{(1,2,3)}$ (or their correct combinations, if the parameters cannot be resolved individually).

The first step in this inversion procedure is determination of the parameters of NMO ellipses—a procedure that may be influenced by nonhyperbolic moveout on finite-spread gathers. However, as shown by Grechka and Tsvankin (1998b) and Grechka et al. (1999), conventional-spread *P*-wave moveout in an orthorhombic layer is typically close to hyperbolic with the moveout (stacking) velocity well approximated by the analytic NMO value from equation (17). The numerical example in Figure 3, performed for spreadlength equal to the CMP-reflector distance, confirms this conclusion for both the horizontal and dipping reflector. The inversion of the two ellipses reconstructed from finite-spread moveout data yields accurate estimates of the η coefficients: $\eta^{(1)} = 0.084$, $\eta^{(2)} = 0.041$, and $\eta^{(3)} = 0.123$ (correct values: 0.1, 0.05 and 0.15, respectively).

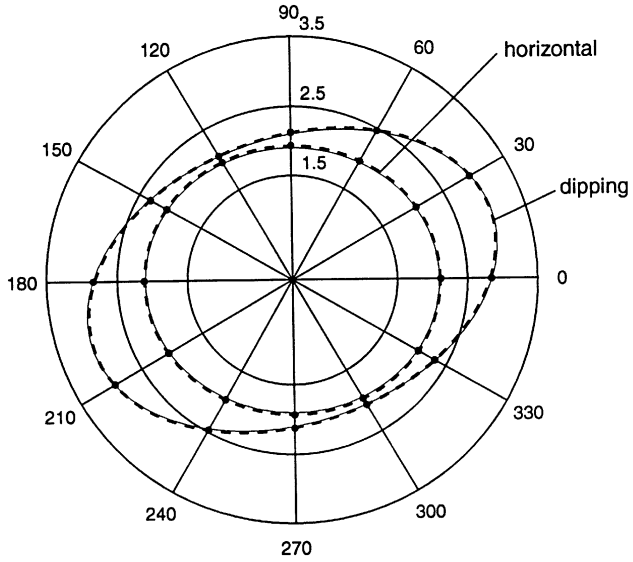

FIG. 3. Comparison of the *P*-wave NMO ellipses for horizontal and dipping events from equations (14) and (17) (thin solid lines) with the moveout (stacking) velocity (dots) obtained by least-squares fitting of a hyperbola to the exact traveltimes computed for speadlength equal to the distance between the CMP and the reflector. The dashed lines mark the best-fit ellipses approximating the measured moveout velocity (i.e., traced through the dots). For the dipping reflector, the azimuth of the dip plane is 30° (azimuth 0° on the plot corresponds to the $[x_1, x_3]$ symmetry plane) and dip is 40°. The layer parameters are $V_{\rm nmo}^{(1)} = 1.90$ km/s, $V_{\rm nmo}^{(2)} = 2.10$ km/s, $\eta^{(1)} = 0.1$, $\eta^{(2)} = 0.05$, $\eta^{(3)} = 0.15$ ($\epsilon^{(1)} = 0.1$, $\epsilon^{(2)} = 0.17$, $\delta^{(1)} = 0$, $\delta^{(2)} = 0.11$, $\delta^{(3)} = -0.16$).

The higher error in the parameter $\eta^{(3)}$ is due to the fact that this coefficient mostly influences near-horizontal velocity variations (see the discussion below).

The results for the model in Figure 3, as well as those for a number of other models we have studied, show that a certain percentage error in the NMO velocity translates into a similar absolute error in the coefficients $\eta^{(1)}$ and $\eta^{(2)}$; the same conclusion was drawn previously for η inversion in VTI media by Alkhalifah and Tsvankin (1995) and Grechka and Tsvankin (1998b). In the example from Figure 3, the maximum error in the NMO velocity for both horizontal and dipping events is smaller than 1.5%. The magnitude of nonhyperbolic moveout for horizontal reflectors increases with $\eta^{(1)}$ and $\eta^{(2)}$, but the associated NMO-velocity error on conventional spreads seldom exceeds 2.5–3%. If the data after hyperbolic moveout correction show residual moveout, it is possible to obtain a more accurate estimate of $V_{\rm nmo}$ by applying a nonhyperbolic moveout equation (Grechka and Tsvankin, 1998a).

The only source of errors in the example from Figure 3 is the influence of nonhyperbolic moveout, which proved to be relatively small. A more general analysis of the influence of errors in the input data is presented in Figure 4. If the components of the matrices **W** are taken from the two exact NMO ellipses, the inversion of equation (28) gives almost perfect results, with

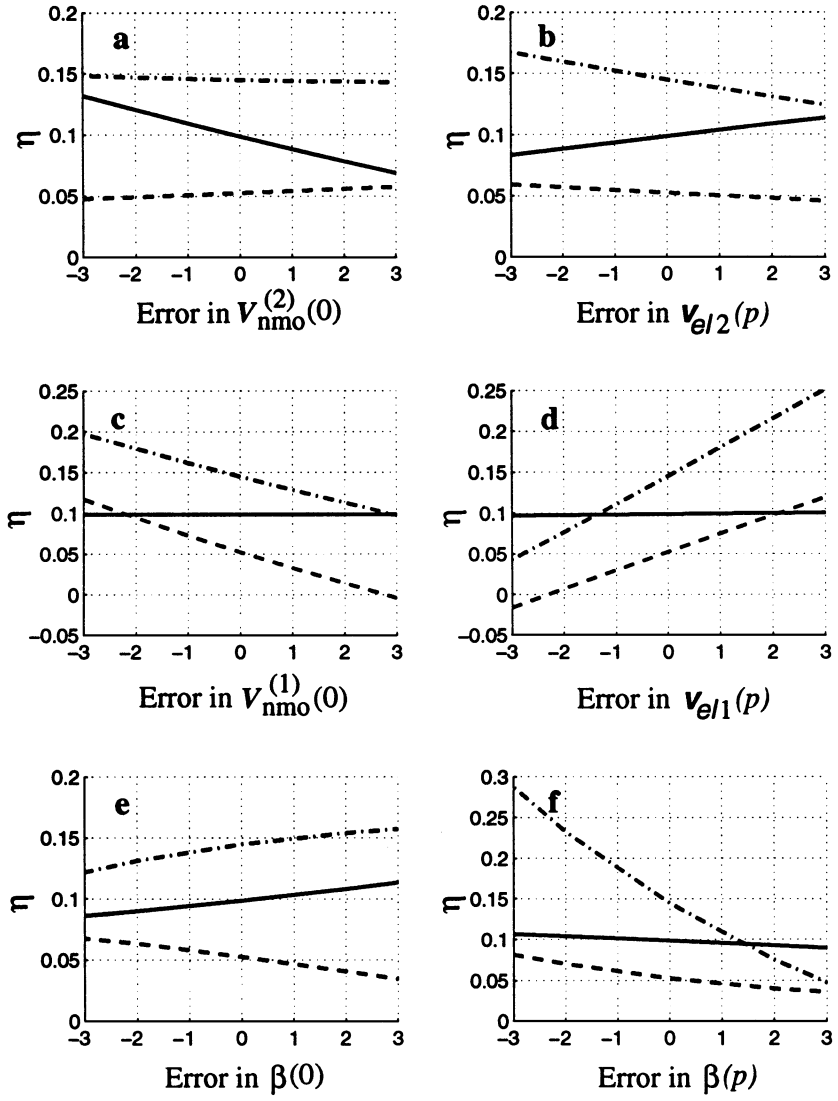

FIG. 4. Inversion of the P-wave NMO ellipses from a horizontal and dipping reflector for $\eta^{(1)}$ (dashed line), $\eta^{(2)}$ (solid line), and $\eta^{(3)}$ (dash-dotted line) in the presence of errors in input data. The dip plane makes an angle of 30° with the $[x_1, x_3]$ symmetry plane, and the dip is 40°. (a) and (c) Errors (in percent) in the semiaxes of the ellipse for the horizontal event; (b) and (d) errors (in percent) in the semiaxes of the ellipse for dipping event; (e) errors (in degrees) in the orientation angle $\beta(0)$ of the NMO ellipse for the horizontal event; (f) errors (in degrees) in the orientation angle $\beta(p)$ of the NMO ellipse for the dipping event. The actual parameters are $\eta^{(1)} = 0.05$, $\eta^{(2)} = 0.10$, and $\eta^{(3)} = 0.15$. The inversion results in the absence of errors: $\eta^{(1)} = 0.053$, $\eta^{(2)} = 0.099$, and $\eta^{(3)} = 0.145$.

the recovered $\eta^{(1,2,3)}$ differing by no more than 0.005 from the actual values. These minor errors are explained by the fact that in the inversion procedure we intentionally used inaccurate values of $V_{P0} = \hat{V} = 2.0$ km/s [see equation (A-11)] (the actual $V_{P0} = 1.9$ km/s) and $V_{S0} = V_{P0}/2 = 0.95$ km/s (the actual $V_{S0} = 0.6$ km/s). This is another illustration of the negligible influence of the vertical velocities (which are generally unknown) on the NMO function; hence, it is justified to use reasonable estimates for V_{P0} and V_{S0} in the inversion procedure.

It is clear from Figure 4 that the various η coefficients are most sensitive to errors in different measured quantities. For instance, $\eta^{(2)}$ (the solid line in Figures 4a,b) strongly depends on the larger semiaxes of both NMO ellipses (which are close to the $[x_1, x_3]$ plane) and is almost insensitive to the changes in the smaller semiaxes (Figures 4c,d). These conclusions are in good agreement with the analytic results obtained in the weak-anisotropy approximation. As indicated by equation (26), $\eta^{(2)}$ is the only anisotropic coefficient that controls the larger semiaxis of the NMO ellipse (i.e., the dip-line NMO velocity) for a reflector with the dip plane parallel to the x_1-axis. The inversion of the dip-line NMO velocity for $\eta^{(2)}$ in this case involves just $V^{(2)}_{\rm nmo}$—the zero-dip NMO velocity in the same (x_1) direction [see equation (27)]. Since for the model in Figure 4 the azimuth of the dip plane is closer to the x_1-axis than to the x_2-axis, $\eta^{(2)}$ remains primarily responsible for the larger semiaxis of the ellipse for the dipping event and is highly sensitive to $V^{(2)}_{\rm nmo}$.

Equation (26) also shows that if $[x_1, x_3]$ represents the dip plane of the reflector, $\eta^{(1)}$ and $\eta^{(3)}$ influence just the strike-line NMO velocity (i.e., the smaller semiaxis of the NMO ellipse), and only as the difference $\eta^{(1)} - \eta^{(3)}$. In addition, note that the NMO velocity in the strike direction depends on $V^{(1)}_{\rm nmo}$ but does not contain $V^{(2)}_{\rm nmo}$ [equation (26)]. This allows us to understand the results of the inversion for $\eta^{(1)}$ and $\eta^{(3)}$ in Figures 4a–d. First, both $\eta^{(1)}$ and $\eta^{(3)}$ are sensitive mostly to the errors in the smaller semiaxis of the NMO ellipse for the dipping event, as well as in $V^{(1)}_{\rm nmo}$. Second, we were able to restore the difference $\eta^{(1)} - \eta^{(3)}$ with a much higher accuracy than either of the coefficients individually (see Figure 4c,d).

The influence of error in the orientation of the ellipses (Figures 4e,f) is more difficult to interpret, but it can also be explained in terms of the general weak-anisotropy approximation (25). Note that the coefficient $\eta^{(3)}$ (but not $\eta^{(1)}$ and $\eta^{(2)}$) is quite sensitive to errors in the orientation of the ellipse for the dipping event.

Overall, if the dip plane of the reflector is closer to the x_1 direction, the coefficient most tightly constrained by P-wave moveout data is $\eta^{(2)}$. This is not surprising since the parameter $\eta^{(2)}$ is fully responsible for the dip-dependent NMO velocity in the $[x_1, x_3]$ plane. In contrast, the coefficient $\eta^{(3)}$ proves to be most sensitive to errors in the input data, especially in the orientation and in the smaller semiaxis of the NMO ellipse for the dipping event. Since $\eta^{(3)}$ is defined in the horizontal symmetry plane, its influence on NMO velocity for moderate reflector dips (e.g., a dip of 40° in Figure 4) is smaller than that of $\eta^{(1)}$ and $\eta^{(2)}$. A more stable estimate of $\eta^{(3)}$ requires the presence of a steeper reflector with the dip plane sufficiently deviating from the vertical symmetry planes.

In summary, the inversion of the P-wave NMO ellipses corresponding to reflections from a horizontal and dipping interface in a homogeneous orthorhombic layer may yield the orientation of the vertical symmetry planes, two symmetry-plane NMO velocities from a horizontal reflector, and three anisotropic parameters $\eta^{(1,2,3)}$. Since the η coefficients control the dip dependence of NMO velocity and make no contribution to moveout for horizontal events, the dipping interface used in the inversion should not be too close to horizontal. In agreement with the results of Alkhalifah and Tsvankin (1995) for η inversion in VTI media, the estimates of the anisotropic parameters become unstable for mild dips below 20–25°.

MOVEOUT INVERSION FOR LAYERED MEDIA

Dix-type layer stripping in orthorhombic media

The inversion approach outlined above can be extended to horizontally layered orthorhombic media above a dipping reflector (Figure 5) using the generalized Dix equation developed by Grechka et al. (1999). As before, it is assumed that we have a minimum of three azimuthal moveout measurements that allow us to reconstruct the effective NMO ellipses [i.e., the matrices $\mathbf{W}(L)$] for reflections from both horizontal and dipping interfaces. Also, we use reflections on the zero-offset sections along the same lines to obtain the horizontal slowness components p_1 and p_2 of the zero-offset ray for the dipping event.

The matrix $\mathbf{W}(L)$ that describes the effective NMO ellipse for data recorded at the surface from a horizontal or dipping

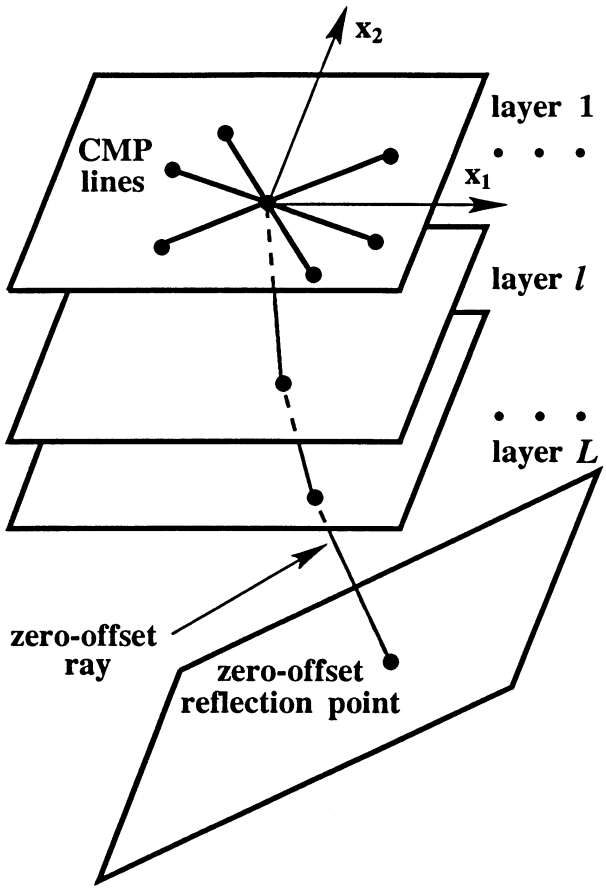

FIG. 5. Horizontally layered orthorhombic medium above a dipping reflector.

reflector can be found by the following averaging of the interval matrices $\mathbf{W}_\ell$ (Grechka et al., 1999):

$$\mathbf{W}^{-1}(L) = \frac{1}{\tau(L)} \sum_{\ell=1}^{L} \tau_\ell \, \mathbf{W}_\ell^{-1}, \qquad (30)$$

where τ_ℓ are the interval zero-offset traveltimes and $\tau(L) = \sum_{\ell=1}^{L} \tau_\ell$. Equation (30) for the effective matrix $\mathbf{W}$ is valid for horizontally layered overburden (Figure 5) with arbitrary symmetry in each layer. It should be emphasized that all interval matrices in equation (30) are evaluated for the horizontal slownesses p_1 and p_2 of the zero-offset ray from the dipping reflector.

Given the effective matrices for reflections from the top and bottom of layer ℓ and the corresponding zero-offset traveltimes, the interval matrix $\mathbf{W}_\ell$ can be obtained by Dix-type differentiation,

$$\mathbf{W}_\ell^{-1} = \frac{\tau(\ell)\mathbf{W}^{-1}(\ell) - \tau(\ell-1)\mathbf{W}^{-1}(\ell-1)}{\tau(\ell) - \tau(\ell-1)}. \qquad (31)$$

Evidently, instead of the squared NMO velocities in the conventional Dix equation, equations (30) and (31) contain the inverse of the matrices $\mathbf{W}$ responsible for the interval NMO ellipses. Only if the model has a throughgoing symmetry plane (i.e., the dip plane coincides with a plane of symmetry in all layers), does equation (30) split into two rms-averaging equations for the NMO velocities in the dip and strike directions (Grechka et al., 1999). In general, however, application of the conventional form of the Dix equation in the presence of azimuthal anisotropy and/or reflector dip leads to errors in the interval values. For instance, as shown in Appendix B, rms averaging of interval NMO velocities at a fixed azimuth always underestimates the effective velocity near intersections of interval NMO ellipses.

In contrast to the conventional Dix equation, the only components of equation (30) that can be obtained from the data directly are the effective matrix $\mathbf{W}(L)$ and the zero-offset travel time $\tau(L)$ for the reflection from the dipping interface. The interval matrices $\mathbf{W}$ in the horizontal layers generally correspond to nonexistent reflectors normal to the slowness vector of the zero-offset ray. Nevertheless, it is still possible to devise a layer-stripping procedure using equation (31), if dipping reflectors (not necessarily with the same dip) are present in each interval.

Here, we develop such a layer-stripping procedure for a stratified orthorhombic medium. First, we carry out the Dix-type differentiation (31) of the NMO ellipses for reflections from horizontal interfaces to obtain the interval matrices $\mathbf{W}_\ell$ for the horizontal events. Since the slowness vector of the zero-offset ray from all horizontal boundaries is vertical ($p_1 = p_2 = 0$), the effective matrices for the top and bottom of each layer needed in equation (31) can be obtained from the data directly, without any recalculation from one ray-parameter value to another. The interval NMO ellipses for horizontal reflectors yield the orientation of the symmetry planes in each layer [described by the rotation angles $\beta_\ell(0)$] and the symmetry-plane NMO velocities $V^{(1)}_{\mathrm{nmo},\ell}$ and $V^{(2)}_{\mathrm{nmo},\ell}$. Note that we do not assume that the medium has throughgoing vertical symmetry planes [i.e., $\beta_\ell(0)$ is not necessarily constant]; the generalized Dix equation allows the orientation of the symmetry planes to vary from layer to layer in an arbitrary fashion.

After performing the Dix-type differentiation for horizontal reflections, we can use dipping events to estimate the interval values of $\eta_\ell^{(1,2,3)}$. The results of the single-layer inversion show that to resolve all three η coefficients in each interval, we need at least one dipping reflector, with the azimuth of the dip plane deviating sufficiently from that of the symmetry planes for this layer. Realistically, we determine the effective values of the anisotropic coefficients between the available velocity picks, whether the corresponding intervals are homogeneous or not.

The inversion procedure in the first (subsurface) layer [equations (28) and (29)] yields the values of $V^{(1)}_{\mathrm{nmo},1}$, $V^{(2)}_{\mathrm{nmo},1}$, $\beta_1(0)$, $\eta_1^{(1)}$, $\eta_1^{(2)}$, and $\eta_1^{(3)}$ that can be used to calculate the interval matrix $\mathbf{W}_1$ for the parameters p_1 and p_2 corresponding to the dipping reflector in the second layer. Then we compute the effective matrix $\mathbf{W}(2)$ from the azimuthally dependent NMO velocity for this dipping reflector (along with the zero-offset traveltime) and apply equation (31) to obtain the interval matrix $\mathbf{W}_2$ in the second layer. Using the interval values $V^{(1)}_{\mathrm{nmo},2}$, $V^{(2)}_{\mathrm{nmo},2}$ found from the horizontal events, the matrix $\mathbf{W}_2$ is inverted for the parameters $\eta_2^{(1)}$, $\eta_2^{(2)}$, and $\eta_2^{(3)}$. This layer-stripping procedure is continued downward, as long as both horizontal and dipping events are available. Note that to calculate the interval matrix in any layer $\mathbf{W}_L$, the matrices $\mathbf{W}_\ell$ in all overlying layers $\ell = 1, \ldots, L-1$ need to be recalculated to the values of p_1 and p_2 for the dipping reflector in layer L.

Implementation of the Dix-type layer-stripping procedure described above requires computing not only the interval matrices $\mathbf{W}_\ell$, but also the interval traveltimes τ_ℓ, as functions of p_1 and p_2. Although P-wave traveltimes in general depend on the vertical velocity and five ϵ and δ coefficients, below we show that the moveout parameters $V^{(1)}_{\mathrm{nmo}}$, $V^{(2)}_{\mathrm{nmo}}$, $\eta^{(1)}$, $\eta^{(2)}$, and $\eta^{(3)}$ are sufficient for converting the vertical zero-offset traveltime $\tau_{0,\ell}$ in a horizontal orthorhombic layer (known from horizontal events) into the traveltime along an arbitrary oblique ray. The one-way traveltime $\tau(p)$ in the ℓth layer (below we omit the index ℓ for brevity) can be calculated as the ratio of the layer thickness z and the vertical component of the group velocity g_3,

$$\tau(p) = \frac{z}{g_3} = \frac{\tau_0 \, V_{P0}}{g_3}, \qquad (32)$$

where τ_0 is the vertical zero-offset traveltime and V_{P0} is the vertical velocity. For the vertical group-velocity component, Grechka et al. (1999) obtained the following equation:

$$g_3 = \frac{1}{q - p_1 q_{,1} - p_2 q_{,2}}, \qquad (33)$$

where, again, $q_{,i}$ are the partial derivatives of the vertical component of slowness $q \equiv p_3$ with respect to the horizontal components p_i. Substituting equation (33) into equation (32) yields

$$\tau(p) = \tau_0 \, V_{P0} \, (q - p_1 q_{,1} - p_2 q_{,2}). \qquad (34)$$

Numerical analysis of equation (34) indicates that the ratio $\tau(p)/\tau_0$ expressed through the parameters p_1 and p_2 is indeed fully controlled by the two NMO velocities and three η coefficients responsible for the NMO-velocity function (Figure 6).

The principle of our layer-stripping procedure is close to that of the 2-D inversion algorithm for η in VTI media, described by Alkhalifah and Tsvankin (1995). Here, however, we operate with NMO ellipses influenced by the 3-D character of wave

propagation, rather than with normal-moveout velocities measured in a vertical symmetry plane of the model.

The stability of the interval parameter estimation is influenced by errors in the single-layer inversion procedure discussed above, as well as by the magnification of errors during the Dix-type differentiation. As in the conventional Dix velocity analysis, the accuracy in the interval values is inversely proportional to the thickness of the interval. Let us denote the relative time thickness of the ℓth layer (for which the differentiation is performed) as

$$\sigma_\ell = \frac{\tau_\ell}{\tau(\ell)}\,. \tag{35}$$

Then equation (31) can be rewritten in the form

$$\mathbf{W}_\ell^{-1} = \frac{1}{\sigma_\ell}\left[\mathbf{W}^{-1}(\ell) - (1-\sigma_\ell)\mathbf{W}^{-1}(\ell-1)\right], \tag{36}$$

which explicitly shows that, for small σ_ℓ, any errors in effective NMO ellipses will propagate into the errors in interval ellipses with the magnification factor $1/\sigma_\ell$.

Synthetic example

We applied our algorithm to the inversion of the exact (ray-traced) reflection traveltimes in a three-layer orthorhombic model having a throughgoing dipping reflector (Figure 7). NMO ellipses for horizontal and dipping events were obtained by hyperbolic semblance analysis for spreadlengths close to and even larger than the CMP-reflector distance. In principle, these estimates may be distorted by the influence of nonhyperbolic moveout that is usually enhanced by vertical inhomogeneity. However, as seen in Figure 8, deviations of the exact traveltimes from the hyperbola parameterized by the analytic NMO velocity become pronounced only for offsets that exceed the distance between the CMP and the reflector. Note that the moveouts shown in Figure 8 are calculated for rays that crossed three orthorhombic layers with different orientation of the vertical symmetry planes and, therefore, bear the full impact of azimuthal anisotropy and vertical inhomogeneity. It is interesting that the magnitude of nonhyperbolic moveout is much more significant for the horizontal reflector, whereas the moveout of the dipping event stays close to the analytic hyperbola up to relatively large offsets. The same conclusion was drawn by Tsvankin (1995) in his study of dip-plane moveout for vertical transverse isotropy. Indeed, if both the spreadlength and the distance between the CMP and the reflector are fixed, the range of take-off angles for reflected rays decreases with dip, which mitigates the influence of anisotropy on the traveltimes and reduces the departure from hyperbolic moveout.

Although the errors in the effective NMO ellipses are somewhat higher (mostly for horizontal events) than those in the single-layer model (Figure 3), the accuracy of our NMO equations is quite sufficient for a stable recovery of the anisotropic parameters (Table 1). The overall maximum error in the η coefficients is slightly over 0.03, with the error in the relatively thin deepest layer of just 0.02. The consistently negative errors in all anisotropic coefficients are explained by the fact that the increasing influence of nonhyperbolic moveout with depth leads to overestimation of the interval NMO velocities from horizontal reflectors. (This interval error, however, is not substantial because the distortion in the NMO velocities from both the top and bottom of each layer has the same sign.) Since the errors in the NMO velocities from dipping reflectors are almost negligible, the overestimates of $V_{\rm nmo}^{(1,2)}$ have to be compensated by underestimates of $\eta^{(1,2,3)}$ to match the NMO ellipses for the dipping events.

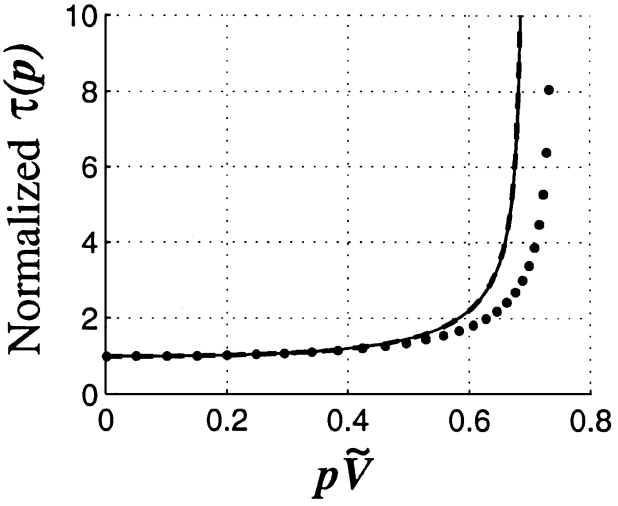

FIG. 6. Dependence of the traveltime $\tau(p)$ along an oblique ray on the parameters of a horizontal orthorhombic layer. The slowness vector is confined to the vertical plane that makes an angle of 30° with the x_1-axis. Models are taken from Figure 2: the solid line is for model 1, the dashed line is for model 2 (the same $V_{\rm nmo}^{(i)}$ and $\eta^{(i)}$ as in model 1 but different $\epsilon^{(i)}$ and $\delta^{(i)}$), and the dotted line is for model 3 (smaller $\eta^{(1)}$ and $\eta^{(2)}$ than in model 1). $\tilde{V}$ is defined by equation (A-11).

P-WAVE TIME PROCESSING IN ORTHORHOMBIC MEDIA

The kinematic equivalence between the symmetry planes of orthorhombic media and vertical transverse isotropy implies that 2-D *P*-wave time processing [i.e., NMO and dip-moveout (DMO) corrections, prestack and poststack time migration] in each vertical symmetry plane of orthorhombic media is controlled solely by the in-plane zero-dip NMO velocity and

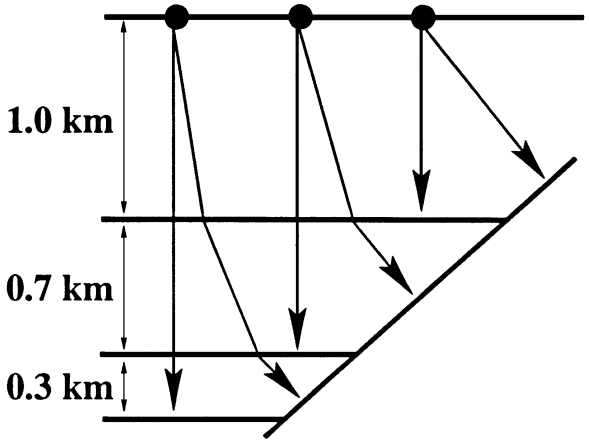

FIG. 7. 2-D sketch of the layered orthorhombic model used to test the inversion algorithm. The azimuth $\beta(0)$ of the $[x_1, x_3]$ symmetry plane changes with depth: layer 1, $\beta_1(0) = 0°$; layer 2, $\beta_2(0) = -10°$; layer 3, $\beta_3(0) = -20°$ (the parameters of each layer are given in Table 1). The azimuth of the dip plane of the reflector is 30°, and the dip is 40°.

the corresponding η coefficient (Tsvankin, 1997). (The 2-D assumption implies that both the rays and their corresponding phase-velocity vectors stay in the vertical symmetry plane, which can happen only if this symmetry plane coincides with the dip plane of the subsurface structure.) The needed parameters for the $[x_1, x_3]$ plane are $V_{\rm nmo}^{(2)}$ and $\eta^{(2)}$, and for the $[x_2, x_3]$ plane the appropriate pair is $V_{\rm nmo}^{(1)}$ and $\eta^{(1)}$.

One can expect that 3-D time processing outside the symmetry planes involves at least one additional parameter: $\eta^{(3)}$ (or $\delta^{(3)}$). Indeed, while normal moveout from horizontal reflectors and, therefore, NMO correction are determined by the symmetry-plane azimuths and two zero-dip NMO velocities $V_{\rm nmo}^{(1)}$ and $V_{\rm nmo}^{(2)}$, NMO velocity for dipping events (and DMO correction) also depends on $\eta^{(1)}$, $\eta^{(2)}$, and $\eta^{(3)}$. In this section, we analyze migration impulse responses and show that poststack time migration in orthorhombic media is governed by the same parameters as is normal moveout. This conclusion is in agreement with the work by Ikelle (1996), who studied the dispersion relation in weakly anisotropic orthorhombic media. It should be emphasized that our results are not limited to weak anisotropy.

The responses displayed in Figures 9 and 10 were computed using the 3-D PSPI (phase-shift-plus-interpolation) migration code developed by Le Rousseau (1997). Models 1 and 2, already used in Figure 2, have vastly different elastic properties but identical parameters $V_{\rm nmo}^{(1)}$, $V_{\rm nmo}^{(2)}$, $\eta^{(1)}$, $\eta^{(2)}$, and $\eta^{(3)}$. The 3-D poststack time-migration impulse responses for these models proved to be practically indistinguishable, both within and outside the symmetry planes; this is illustrated in Figure 9 for a vertical section making an angle of 30° with the x_1-axis. The same results were obtained in other tests performed for a representative set of orthorhombic models.

Any variation in the relevant parameters leads to changes in the shape of the migration impulse response. For instance, a decrease in $\eta^{(1)}$ and $\eta^{(2)}$ translates into smaller horizontal velocities and thus narrower impulse response (Figure 10).

Since both normal moveout (i.e., NMO and DMO) and poststack time migration are fully controlled by the symmetry-plane orientation, zero-dip NMO velocities $V_{\rm nmo}^{(1)}$ and $V_{\rm nmo}^{(2)}$, and the anisotropic coefficients $\eta^{(1)}$, $\eta^{(2)}$ and $\eta^{(3)}$, these parameters are responsible for the whole P-wave 3-D time-processing sequence. Consequently, the same set of parameters is sufficient for prestack time migration. P-wave depth processing, however, requires knowledge of the vertical velocity and all ϵ and δ coefficients (a total of six parameters).

DISCUSSION AND CONCLUSIONS

We have shown that the exact P-wave normal-moveout velocity in orthorhombic media is fully controlled by the orientation of the vertical symmetry planes and five medium parameters: two symmetry-plane NMO velocities for reflections from a horizontal interface ($V_{\rm nmo}^{(1)}$ and $V_{\rm nmo}^{(2)}$) and three anisotropic coefficients ($\eta^{(1)}$, $\eta^{(2)}$, and $\eta^{(3)}$). The parameters $\eta^{(1)}$ and $\eta^{(2)}$ are introduced in the vertical symmetry planes by analogy with the Alkhalifah-Tsvankin "anellipticity" coefficient η for vertical transverse isotropy, and $\eta^{(3)}$ is a similar parameter defined in the horizontal symmetry plane [in principle, it can be replaced with the original Tsvankin's (1997) coefficient $\delta^{(3)}$].

Table 1. Comparison of the inverted and actual values of the interval parameters for the three-layer orthorhombic model from Figure 7.*

	Correct values						Inverted values					
Layer	$V_{\rm nmo}^{(1)}$ (km/s)	$V_{\rm nmo}^{(2)}$ (km/s)	β (°)	$\eta^{(1)}$	$\eta^{(2)}$	$\eta^{(3)}$	$V_{\rm nmo}^{(1)}$ (km/s)	$V_{\rm nmo}^{(2)}$ (km/s)	β (°)	$\eta^{(1)}$	$\eta^{(2)}$	$\eta^{(3)}$
1	2.50	2.76	0.0	0.10	0.05	0.15	2.54	2.79	0.0	0.07	0.04	0.13
2	2.90	3.18	−10.0	0.15	0.10	0.15	2.97	3.23	−8.0	0.12	0.08	0.13
3	3.20	3.77	−20.0	0.20	0.15	0.20	3.25	3.83	−18.0	0.18	0.13	0.18

*The maximum source-receiver offsets used in estimating moveout velocity are as follows: horizontal and dipping reflectors in layer 3 = 1.8 km (spreadlength-to-depth ratio $X_{\max}/D = 0.9$); layer 2 = 1.8 km ($X_{\max}/D = 1.06$); layer 1 = 1.2 km ($X_{\max}/D = 1.2$).

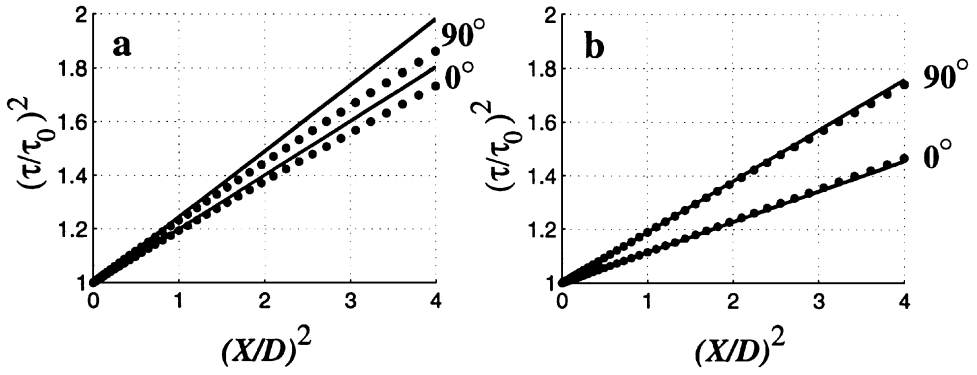

FIG. 8. Accuracy of the hyperbolic moveout equation for the model from Figure 7. Dots show P-wave traveltimes computed by 3-D anisotropic ray tracing; solid lines are hyperbolic moveout curves parameterized by the NMO velocity calculated using the generalized Dix equation (30). (a) Reflection from the deepest horizontal boundary (bottom of layer 3); (b) reflection from the segment of the dipping interface in layer 3. τ is the traveltime, X is the source-receiver offset, $\tau_0 = \tau(X = 0)$; D is the distance between the CMP and the reflector.

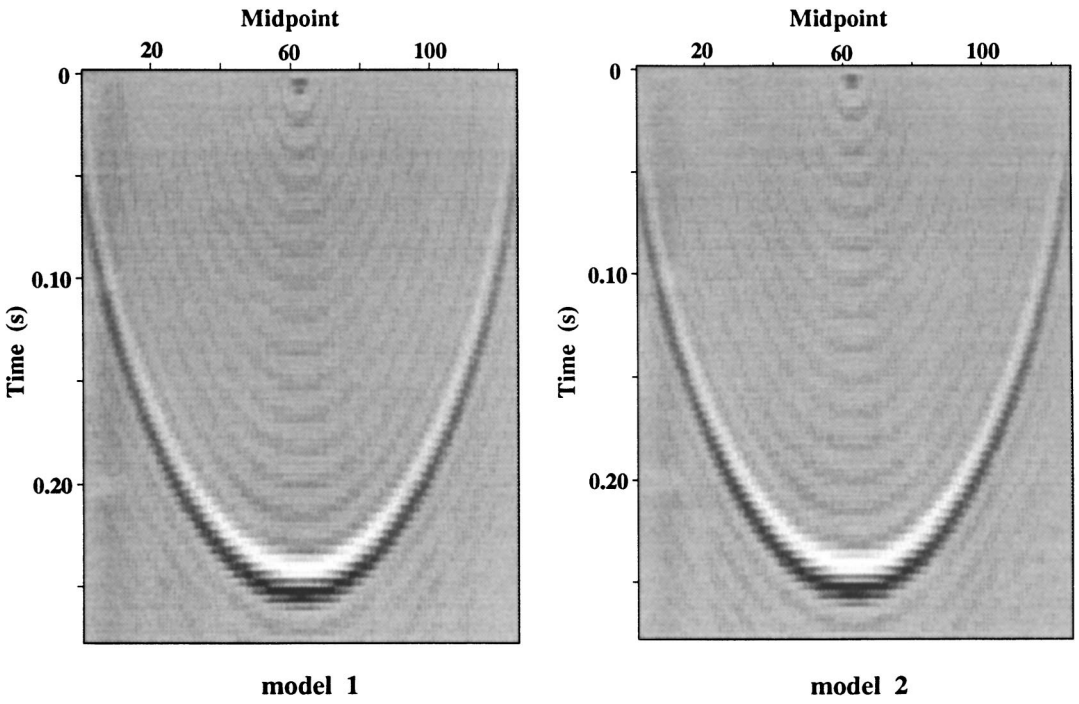

FIG. 9. Impulse response of 3-D poststack time migration in the vertical plane that makes an angle of 30° with the $[x_1, x_3]$ symmetry plane. Models are taken from Figure 2; model 2 has the same $V_{\mathrm{nmo}}^{(i)}$ and $\eta^{(i)}$ as in model 1 but different $\epsilon^{(i)}$ and $\delta^{(i)}$.

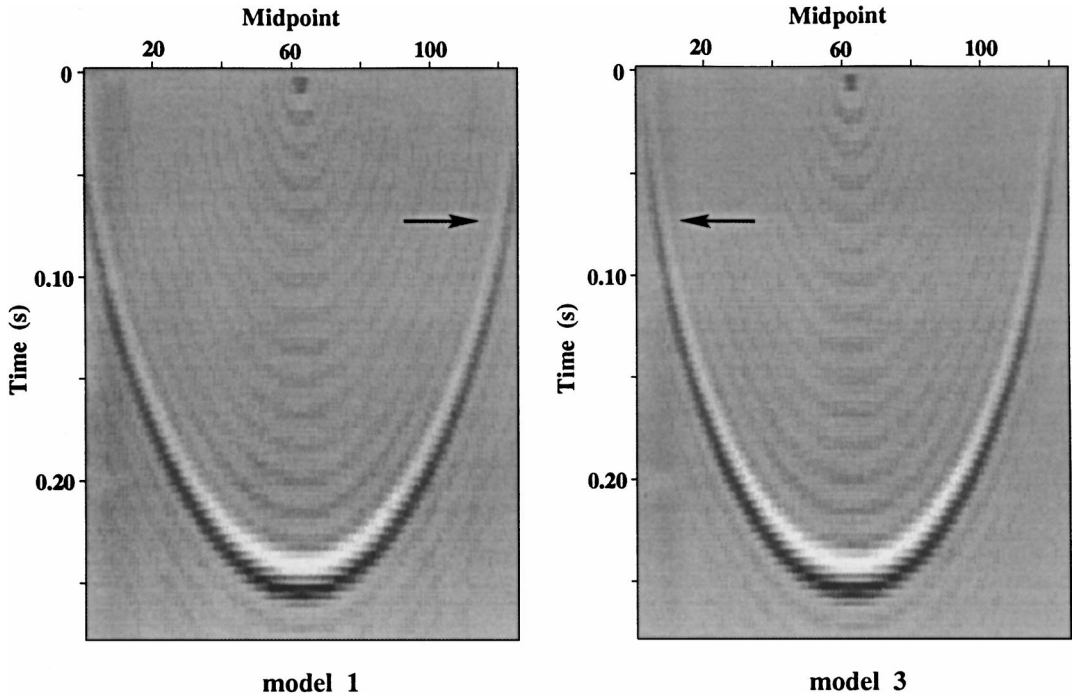

FIG. 10. The influence of the η coefficients on the time-migration impulse response. The plot for model 1 is reproduced from Figure 9. Model 3 has the same parameters as model 1, except for $\eta^{(1)} = 0.1$ and $\eta^{(2)} = 0.2$. Note the difference in the responses near horizontal (arrows).

The velocities $V_{\rm nmo}^{(1)}$ and $V_{\rm nmo}^{(2)}$ are responsible for normal moveout from horizontal reflectors, while $\eta^{(1,2,3)}$ determine the dip dependence of NMO velocity. It should be emphasized that the above parameters govern the NMO function expressed through the horizontal slowness components of the zero-offset ray (rather than the dip and azimuth of the reflector normal)—quantities that can be obtained from reflection slopes on zero-offset sections.

The parameters identified in our study of the NMO function proved to be of crucial importance in time migration as well. By using the phase-shift (PSPI) migration algorithm of Le Rousseau (1997), we showed that 3-D poststack time migration for orthorhombic anisotropy is controlled by the same parameters as is normal moveout. Therefore, the orientation of the symmetry planes, two zero-dip NMO velocities and three η coefficients are fully responsible for all 3-D P-wave time-processing steps (NMO correction, DMO removal, prestack and poststack time migration) in orthorhombic media. Depth processing, however, requires knowledge of all six parameters that determine P-wave kinematic signatures in orthorhombic media: the vertical velocity and five ϵ and δ coefficients.

All time-processing parameters can be obtained from normal-moveout velocities of horizontal and dipping events (i.e., from surface P-wave data alone). We developed a moveout-inversion procedure for horizontally layered orthorhombic media above a dipping reflector using the analytic representation of NMO velocity given by Grechka and Tsvankin (1998b) and by Grechka et al. (1999). For any pure mode, the azimuthal dependence of NMO velocity is governed by three parameters and typically has an elliptical shape in the horizontal plane (Grechka and Tsvankin, 1998b). Hence, a minimum of three azimuthal moveout measurements (e.g., available in "wide-azimuth" 3-D surveys; Corrigan et al., 1996) is required to reconstruct the NMO ellipse for a given reflection event. Then, the three coefficients of the ellipse (e.g., its semiaxes and the orientation angle) can be inverted for the relevant combinations of the medium parameters.

First, we studied the inversion of reflection traveltimes from horizontal and dipping reflectors in a single orthorhombic layer. The NMO ellipse for horizontal events yields the orientation of the vertical symmetry planes and the velocities $V_{\rm nmo}^{(1)}$ and $V_{\rm nmo}^{(2)}$. Then, we used normal moveout of at least one dipping event along with the obtained values of $V_{\rm nmo}^{(1,2)}$ to find the coefficients $\eta^{(1)}$, $\eta^{(2)}$, and $\eta^{(3)}$. Since $\eta^{(1,2,3)}$ control the dip-dependence of NMO velocity and make no contribution to moveout for horizontal events, the dip used in the inversion should not be too mild. The presence of a sufficient dip, however, does not guarantee the recovery of all three η parameters. If the dip-plane azimuth is close to the $[x_1, x_3]$ symmetry plane, one can resolve only the coefficient $\eta^{(2)}$ (defined in this plane) and the difference $(\eta^{(1)} - \eta^{(3)})$. Likewise, if the dip line is close to the $[x_2, x_3]$ plane, the inversion yields the parameter $\eta^{(1)}$ and the difference $(\eta^{(2)} - \eta^{(3)})$. Estimation of the individual values of all three coefficients becomes reasonably stable if the reflector azimuth makes an angle of 20–25° or more with the nearest symmetry plane. For dips up to about 50°, the sensitivity to the errors in input data is higher for $\eta^{(3)}$ than for the other two coefficients because this parameter is largely determined by near-horizontal velocity variations outside the vertical symmetry planes.

Extension of our inversion scheme to vertically inhomogeneous media is based on the generalized Dix equation (Grechka et al., 1999), which operates with the matrices responsible for interval NMO ellipses. For horizontal events, our procedure is similar to the conventional Dix differentiation because the effective NMO ellipses corresponding to the reflections from the top and bottom of each horizontal layer can be obtained from the data directly. In the case of dipping events, however, it is necessary to carry out a full-scale layer-stripping procedure by recalculating the NMO ellipses and zero-offset traveltimes in the overburden to the ray-parameter values corresponding to the dipping reflector. As a result of the layer stripping, we obtain the orientation of symmetry planes and the five relevant parameters ($V_{\rm nmo}^{(1)}$, $V_{\rm nmo}^{(2)}$, $\eta^{(1)}$, $\eta^{(2)}$, and $\eta^{(3)}$) in each layer. Our algorithm is subject to the same trade-off between accuracy and resolution as is conventional Dix differentiation (i.e., the accuracy increases with the relative time-thickness of the interval).

We tested our inversion method on a synthetic data set generated by ray tracing in a three-layer orthorhombic model with pronounced anisotropy and depth-varying orientation of the vertical symmetry planes. Despite the presence of nonhyperbolic moveout caused by both heterogeneity and anisotropy, we were able to reconstruct the NMO ellipses on conventional-length spreads with sufficient accuracy and obtain good estimates of the interval values of all parameters.

Our modeling shows that moveout of dipping events remains close to hyperbolic on surprisingly long spreads, twice as large as the CMP-reflector distance. In contrast, traveltimes of horizontal events start to deviate noticeably from a hyperbola for offsets exceeding the reflector depth. These deviations indicate that nonhyperbolic moveout from horizontal reflectors can be included in the inversion for the medium parameters (Sayers and Ebrom, 1997). If the hyperbolic moveout correction does not fully flatten the data, a more reliable estimate of the NMO velocity can be obtained by using a nonhyperbolic moveout equation (Tsvankin and Thomsen, 1994; Grechka and Tsvankin, 1998a).

ACKNOWLEDGMENTS

We are grateful to members of A(nisotropy)-team of the Center for Wave Phenomena (CWP), Colorado School of Mines, for helpful discussions and to Jérôme Le Rousseau (Elf Acquitaine/CWP) for generating migration impulse responses with his PSPI code. We also appreciate reviews of the manuscript by Ken Larner (CWP) and Dennis Corrigan (ARCO). The support for this work was provided by the members of the Consortium Project on Seismic Inverse Methods for Complex Structures at CWP and by the United States Department of Energy.

REFERENCES

Alkhalifah, T., and Tsvankin, I., 1995, Velocity analysis in transversely isotropic media: Geophysics, **60**, 1550–1566.

Cohen, J. K., 1997, Analytic study of the effective parameters for determination of the NMO velocity function in transversely isotropic media: Geophysics, **62**, 1855–1866.

Corrigan, D., Withers, R., Darnall, J., and Skopinski, T., 1996, Fracture mapping from azimuthal velocity analysis using 3D surface seismic data: 66th Ann. Internat. Mtg., Soc. Expl. Geophys., Expanded Abstracts, 1834–1837.

Grechka, V., and Tsvankin, I., 1998a, Feasibility of nonhyperbolic moveout inversion in transversely isotropic media: Geophysics, **63**, 957–969.
——— 1998b, 3-D description of normal moveout in anisotropic inhomogeneous media: Geophysics, **63**, 1079–1092.
Grechka, V., Tsvankin, I., and Cohen, J. K., 1999, Generalized Dix equation and analytic treatment of normal-moveout velocity for anisotropic media: Geophys. Prosp. **47**, 117–148.
Le Rousseau, J., 1997, Depth migration in heterogeneous, transversely isotropic media with the phase-shift-plus-interpolation method: 67th Ann. Internat. Mtg., Soc. Expl. Geophys., Expanded Abstracts, 1703–1706.
Hubral, P., and Krey, T., 1980, Interval velocities from seismic reflection measurements: Soc. Expl. Geophys.
Ikelle, L. T., 1996, Anisotropic migration-velocity based on inversion of common azimuthal sections: J. Geophys. Res., **101**, No. B10, 22461–22484.
Rommel, B., and Tsvankin, I., 1997, Analytic approximations for *P*-wave velocities and polarization in orthorhombic media: Colorado School of Mines Center for Wave Phenomena Research Report (CWP–257).
Sayers, C. M., and Ebrom, D. A., 1997, Seismic traveltime analysis for azimuthally anisotropic media: Theory and experiment: Geophysics, **62**, 1570–1582.
Schoenberg, M., and Helbig, K., 1997, Orthorhombic media: Modeling elastic wave behavior in a vertically fractured earth: Geophysics, **62**, 1954–1974.
Thomsen, L., 1986, Weak elastic anisotropy: Geophysics, **51**, 1954–1966.
Tsvankin, I., 1995, Normal moveout from dipping reflectors in anisotropic media: Geophysics, **60**, 268–284.
——— 1996, *P*-wave signatures and notation for transversely isotropic media: An overview: Geophysics, **61**, 467–483.
——— 1997, Anisotropic parameters and *P*-wave velocity for orthorhombic media: Geophysics, **62**, 1292–1309.
Tsvankin, I., and Thomsen, L., 1994, Nonhyperbolic reflection moveout in anisotropic media: Geophysics, **59**, 1290–1304.
Wild, P., and Crampin, S., 1991, The range of effects of azimuthal isotropy and EDA anisotropy in sedimentary basins: Geophys. J. Internat., **107**, 513–529.

APPENDIX A

WEAK-ANISOTROPY APPROXIMATION FOR *P*-WAVE NMO VELOCITY IN AN ORTHORHOMBIC LAYER

Here, we derive the weak-anisotropy approximation for *P*-wave normal-moveout velocity by linearizing the exact NMO equation (17) in the anisotropic coefficients. Then, we analyze this expression in the dip plane of the reflector and show that it is equivalent to the approximation for the NMO velocity in VTI media given by Alkhalifah and Tsvankin (1995).

General case

The linearized expression for the vertical slowness q, obtained from the Christoffel equation, is given in the main text [equation (20)]. Differentiating equation (20) with respect to p_1 and p_2, substituting the results into equation (17), and further linearizating the NMO equation in the coefficients $\eta^{(1,2,3)}$ yields (we used Mathematica software)

$$V_{\rm nmo}^{-2}(\alpha, p_1, p_2) = \cos^2\alpha \left\{ \left[V_{\rm nmo}^{(2)}\right]^{-2} - p_1^2 + \sum_{i=1}^{3} d_{1i}\,\eta^{(i)} \right\} + 2\sin\alpha\cos\alpha \left\{ -p_1 p_2 + \sum_{i=1}^{3} d_{2i}\,\eta^{(i)} \right\} + \sin^2\alpha \left\{ \left[V_{\rm nmo}^{(1)}\right]^{-2} - p_2^2 + \sum_{i=1}^{3} d_{3i}\,\eta^{(i)} \right\}, \quad \text{(A-1)}$$

where $\eta^{(i)}$ are the linearized anisotropic coefficients from equations (20)–(24), and d_{ki} are given by

$$d_{11} = -2p_2^2\left(1 - 4p_1^2\tilde{V}^2\right)\left(1 - p_1^2\tilde{V}^2 - p_2^2\tilde{V}^2\right), \quad \text{(A-2)}$$

$$d_{12} = -2\left(6p_1^2 + p_2^2 - 9p_1^4\tilde{V}^2 - 5p_1^2p_2^2\tilde{V}^2 + 4p_1^6\tilde{V}^4 + 4p_1^4p_2^2\tilde{V}^4\right), \quad \text{(A-3)}$$

$$d_{13} = 2p_2^2\left(1 - 5p_1^2\tilde{V}^2 + 4p_1^4\tilde{V}^4\right), \quad \text{(A-4)}$$

$$d_{21} = -4p_1p_2\left(1 - 2p_2^2\tilde{V}^2\right)\left(1 - p_1^2\tilde{V}^2 - p_2^2\tilde{V}^2\right), \quad \text{(A-5)}$$

$$d_{22} = -4p_1p_2\left(1 - 2p_1^2\tilde{V}^2\right)\left(1 - p_1^2\tilde{V}^2 - p_2^2\tilde{V}^2\right), \quad \text{(A-6)}$$

$$d_{23} = 4p_1p_2\left(1 - p_1^2\tilde{V}^2 - p_2^2\tilde{V}^2 + 2p_1^2p_2^2\tilde{V}^4\right), \quad \text{(A-7)}$$

$$d_{31} = -2\left(6p_2^2 + p_1^2 - 9p_2^4\tilde{V}^2 - 5p_1^2p_2^2\tilde{V}^2 + 4p_2^6\tilde{V}^4 + 4p_1^2p_2^4\tilde{V}^4\right), \quad \text{(A-8)}$$

$$d_{32} = -2p_1^2\left(1 - 4p_2^2\tilde{V}^2\right)\left(1 - p_1^2\tilde{V}^2 - p_2^2\tilde{V}^2\right), \quad \text{(A-9)}$$

$$d_{33} = 2p_1^2\left(1 - 5p_2^2\tilde{V}^2 + 4p_2^4\tilde{V}^4\right). \quad \text{(A-10)}$$

The parameter $\tilde{V}$ is chosen as

$$\tilde{V} = \tfrac{1}{2}\left(V_{\rm nmo}^{(1)} + V_{\rm nmo}^{(2)}\right), \quad \text{(A-11)}$$

where $V_{\rm nmo}^{(1,2)}$ are the semiaxes of the NMO ellipse from the horizontal reflector linearized in the anisotropic coefficients $\delta^{(i)}$ [equations (15)]:

$$V_{\rm nmo}^{(i)} = V_{P0}\sqrt{1 + 2\,\delta^{(i)}} \approx V_{P0}\left(1 + \delta^{(i)}\right), \qquad (i = 1, 2). \quad \text{(A-12)}$$

There is some flexibility in defining the parameter $\tilde{V}$ which reduces to V_{P0} for isotropic media. Note that $\tilde{V}$ appears only in equations (A-2)–(A-10) for the coefficients d_{ki} that are multiplied by the small quantities $\eta^{(i)}$ in equation (A-1). Therefore, in the linearized weak-anisotropy approximation, we can add any anisotropic terms to $\tilde{V}$ without changing the final result:

$$\tilde{V} = V_{P0}\left[1 + f\left(\epsilon^{(i)}, \delta^{(i)}, \eta^{(i)}\right)\right], \quad \text{(A-13)}$$

where $f(\epsilon^{(i)}, \delta^{(i)}, \eta^{(i)})$ is an arbitrary combination of the anisotropic coefficients that goes to zero in isotropic media. Our choice of $\tilde{V}$ emphasizes the fact that the linearized NMO equation can be represented as a function of just five medium parameters [$V_{\rm nmo}^{(1,2)}$ and $\eta^{(1,2,3)}$], while the individual values of the ϵ and δ coefficients influence only quadratic and higher-order terms.

NMO velocity in the dip plane

Since the slowness vector of the zero-offset ray is normal to the reflecting interface, it is confined to the dip plane of the reflector. Hence, the horizontal components of the slowness

vector can be expressed through the azimuth ν of the dip plane as $p_1 = p\cos\nu$ and $p_2 = p\sin\nu$ ($p = \sqrt{p_1^2 + p_2^2}$ is the horizontal slowness). Substitution of these values of p_1 and p_2 into equation (A-1) yields the following weak-anisotropy approximation for the NMO velocity in the dip direction:

$$V_{\rm nmo}^{-2}(\nu, p) = V_{\rm nmo}^{-2}(\nu, 0) - p^2 - 2p^2\,\bar{\eta}(\nu) \times (4p^4\tilde{V}^4 - 9p^2\tilde{V}^2 + 6), \qquad \text{(A-14)}$$

where

$$\bar{\eta}(\nu) = \eta^{(1)}\,\sin^2\nu + \eta^{(2)}\,\cos^2\nu - \eta^{(3)}\,\sin^2\nu\,\cos^2\nu. \qquad \text{(A-15)}$$

Since $\tilde{V}$ can be replaced by $V_{\rm nmo}(\nu, 0)$, equation (A-14) coincides with the linearized expression for the dip-line NMO velocity in a VTI medium with the zero-dip NMO velocity $V_{\rm nmo}(\nu, 0)$ and parameter $\eta = \bar{\eta}(\nu)$ [Alkhalifah and Tsvankin, 1995; also, see equation (27) of the main text].

To understand the meaning of $\bar{\eta}(\nu)$, we express the weak-anisotropy approximation for P-wave phase velocity [equation (19)] as a function of azimuth ν and the phase angle θ with vertical (Tsvankin, 1997):

$$V_P(\theta, \nu) = V_{P0}\,[1 + \delta(\nu)\sin^2\theta\cos^2\theta + \epsilon(\nu)\sin^4\theta]; \qquad \text{(A-16)}$$

$$\delta(\nu) = \delta^{(1)}\sin^2\nu + \delta^{(2)}\cos^2\nu,$$
$$\epsilon(\nu) = \epsilon^{(1)}\sin^4\nu + \epsilon^{(2)}\cos^4\nu + \left(2\epsilon^{(2)} + \delta^{(3)}\right)\sin^2\nu\,\cos^2\nu.$$

Equation (A-16) has exactly the same form as Thomsen's (1986) weak-anisotropy approximation for vertical transverse isotropy, but with azimuthally dependent coefficients ϵ and δ. Therefore, for any vertical plane $\nu = \text{const}$ in weakly orthorhombic media, in-plane P-wave kinematic signatures can be described by the VTI equations. The linearized VTI parameter η at azimuth ν is given by

$$\eta(\nu) = \epsilon(\nu) - \delta(\nu) = \eta^{(1)}\sin^2\nu + \eta^{(2)}\cos^2\nu - \eta^{(3)}\sin^2\nu\cos^2\nu,$$

which coincides with the coefficient $\bar{\eta}(\nu)$ from equations (A-14) and (A-15).

Therefore, the NMO velocity in the dip plane of the reflector can be obtained from the weak-anisotropy approximation for a VTI medium with the parameters $\epsilon(\nu)$ and $\delta(\nu)$ corresponding to the dip-plane azimuth. This result becomes obvious if we recall that for the CMP line in the dip direction, the reflected rays deviate from the incidence (vertical) plane only due to the influence of azimuthal anisotropy. Evidently, in the linear weak-anisotropy approximation, out-of-plane phenomena can be neglected and rays can be assumed to propagate in the dip plane where all P-wave kinematic signatures (including NMO velocity) are identical to those in VTI media. The analogy with vertical transverse isotropy, however, is limited to the dip plane of the reflector and cannot be applied to CMP lines with any other direction.

APPENDIX B

EFFECTIVE NMO VELOCITY NEAR INTERSECTIONS OF INTERVAL NMO ELLIPSES

As discussed by Grechka et al. (1999), the averaging of the matrices $\mathbf{W}$ in the generalized Dix equation (30) is different from the conventional rms averaging of NMO velocities measured in a fixed azimuthal direction. In this appendix, we illustrate this difference by examining the effective NMO velocity near intersections of interval NMO ellipses.

Let us consider a two-layer model with intersecting NMO-velocity ellipses [see equation (10)]:

$$V_{{\rm nmo},i}^{-2}(\alpha) = W_{11,i}\cos^2\alpha + 2\,W_{12,i}\sin\alpha\cos\alpha + W_{22,i}\sin^2\alpha\,, \qquad (i = 1, 2) \qquad \text{(B-1)}$$

and the corresponding effective ellipse [equation (30)]:

$$\mathbf{U}^{-1} = \frac{1}{\tau_1 + \tau_2}\left(\tau_1\mathbf{W}_1^{-1} + \tau_2\mathbf{W}_2^{-1}\right), \qquad \text{(B-2)}$$

where τ_1 and τ_2 are interval zero-offset traveltimes. Without loss of generality, we can assume that the coordinate system has been chosen in such a way that the ellipses (B-1) intersect (or touch) each other at azimuth $\alpha = 0$, which implies that

$$W_{11,1} = W_{11,2} = W_{11}. \qquad \text{(B-3)}$$

Clearly, conventional rms averaging of NMO velocities at $\alpha = 0$ yields the effective velocity

$$V_{\rm rms,eff}^2(0) = \frac{1}{W_{11}}. \qquad \text{(B-4)}$$

Here, we compare $V_{\rm rms,eff}(0)$ with the exact effective NMO velocity in the same direction ($\alpha = 0$) that can be obtained from equation (B-2) as

$$V_{\rm ex,eff}^2(0) = \frac{1}{U_{11}}. \qquad \text{(B-5)}$$

Substituting equations (B-1) into equation (B-2), we find

$$\frac{V_{\rm ex,eff}^2(0)}{V_{\rm rms,eff}^2(0)} - 1 = \frac{\tau_1\tau_2\,(W_{12,1} - W_{12,2})^2}{(\tau_1 + \tau_2)\,(\tau_1\det\mathbf{W}_2 + \tau_2\det\mathbf{W}_1)}. \qquad \text{(B-6)}$$

Since the interval matrices $\mathbf{W}_i$ are positive definite (Grechka and Tsvankin, 1998b), both determinants in the denominator are positive, and the right-hand side of equation (B-6) is nonnegative. Hence,

$$V_{\rm ex,eff}(0) \geq V_{\rm rms,eff}(0), \qquad \text{(B-7)}$$

i.e., the rms averaging of the interval NMO velocities always underestimates the effective velocity at an intersection of the NMO ellipses.

As a simple example, let us consider a model that consists of two identical horizontal orthorhombic layers with interchanged vertical symmetry planes. The interval ellipses (solid and dashed lines) in such a model are identical but rotated with

respect to each other by 90° (Figure B-1). The effective NMO ellipse (dotted line in Figure B-1) in this case is a circle because the effective NMO velocities in both symmetry planes coincide with each other.

Let us compare the exact effective NMO velocity and the rms-averaged value in the direction $\alpha = \pi/4$. For $\alpha = \pi/4$, the two interval NMO velocities are equal to each other and, therefore, to their rms average [see equation (B-1) with $W_{12} = 0$]:

$$\frac{1}{V^2_{\text{rms,eff}}(\pi/4)} = \frac{1}{2}\left(\frac{1}{\left[V^{(1)}_{\text{nmo}}\right]^2} + \frac{1}{\left[V^{(2)}_{\text{nmo}}\right]^2}\right), \qquad \text{(B-8)}$$

where $V^{(i)}_{\text{nmo}}$ are the interval NMO velocities in the symmetry planes. Therefore, the squared rms velocity at $\alpha = \pi/4$ represents the harmonic average of the squared semiaxes of the interval NMO ellipse.

Since the exact effective NMO velocity in this model is circular, at $\alpha = \pi/4$ it is equal to the values at the symmetry planes ($\alpha = 0$ or $\alpha = \pi/2$), which can be found by conventional rms averaging (Grechka et al., 1999):

$$V^2_{\text{ex,eff}}(\pi/4) = \tfrac{1}{2}\left(\left[V^{(1)}_{\text{nmo}}\right]^2 + \left[V^{(2)}_{\text{nmo}}\right]^2\right). \qquad \text{(B-9)}$$

Thus, the exact squared NMO velocity $V_{\text{ex,eff}}(\pi/4)$ is the arithmetic average of $[V^{(1)}_{\text{nmo}}]^2$ and $[V^{(2)}_{\text{nmo}}]^2$. According to the relation between the harmonic and arithmetic averages,

$$V_{\text{ex,eff}}\,(\pi/4) \geq V_{\text{rms,eff}}\,(\pi/4), \qquad \text{(B-10)}$$

in agreement with the general equation (B-7).

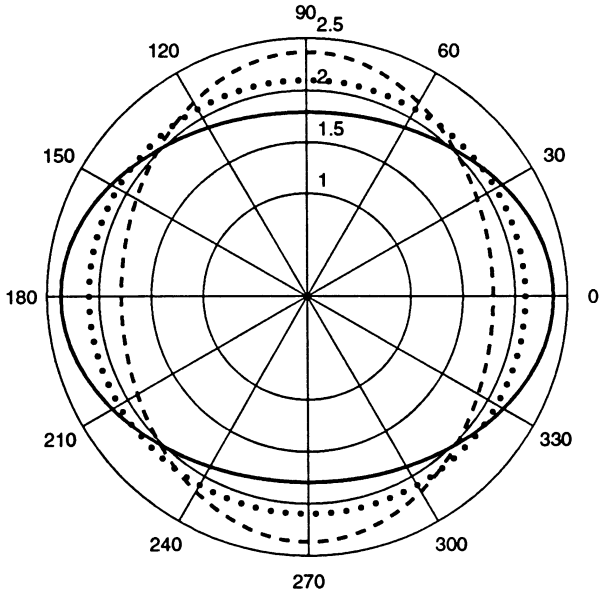

FIG. B-1. The interval P-wave NMO ellipses (solid and dashed) and the effective NMO ellipse (dotted) in a two-layer orthorhombic model. Both layers are horizontal, have the same thickness $z_1 = z_2 = 1.0$ km and the same elastic parameters, but their vertical symmetry planes are rotated by 90° with respect to each other. The vertical velocity $V_{P0,1} = V_{P0,2} = 2.0$ km/s. The parameters δ that control the NMO velocity in the symmetry planes are interchanged: $\delta^{(1)}_1 = -0.1$, $\delta^{(2)}_1 = 0.2$, and $\delta^{(1)}_2 = 0.2$, $\delta^{(2)}_2 = -0.1$.